Author's replies to Referees comments

The authors would like to thanks all referees for the useful and constructive criticism. We tried to address all the referees comments and requests and to modify the manuscript accordingly.

Following are the replies (in italics) to each referee comment (in bold)

Referee #1

R1C: The authors present an interesting and relevant set of observations. Their paper can eventually make a fine contribution to the literature. I have a generally favorable view of the analysis. However, while the analysis of circulation patterns and water masses are thorough and well done, I see significant problems with the analysis of the turbulent dissipation rates. In essence, although with modifications, the authors claim that "TKE dissipation rates follow closely the similarity scaling for wind stress generated turbulence and for the one due to bottom shear stress near the sea floor (Fig. 8)." However, in a substantial number of profiles, epsilon deviates by an order of magnitude or more from similarity scaling. Specifically, epsilon appears systematically elevated over similarity values toward the surface (upper 7-12 m). Some of these instances are not addressed by the authors. The analysis is carried out solely in terms of boundary forcing with modifications due to stable stratification.

AC: In the revised manuscript we addressed the surface mismatch between scaling and observation by including in our analysis the role of waves in surface turbulence generation. Since we did not collected continuous wave observations during the yoyo casts we relayed on the VIDA buoy data to produce a regime diagram to analyse the relationship of turbulence forcing. Although the surface turbulence scaling is a very interesting topic we think that the collected data do not through study of such issue and hence we focus our analysis on the lower part of the water column.

R1C: The text is also somewhat hard to follow.

AC: The structure of the paper was significantly modified, specifically the manuscript is now structured as follows

Abstract,

1 *Introduction*

2 *Observations and data processing*

2.1 *Meteorological conditions and surface forcing*

2.2 *Hydrological conditions and water mass structur*

3 *Turbulence scaling*

4 *Yoyo casts and turbulence observations*

5 *Summary and discussion*

Appendix A

The manuscript grammar and syntax was checked and improved.

R1C: In my view the analysis of the turbulent mixing is not very statisfactory and insufficient. I recommend a wider perspective that should include the effects of surface waves, Langmuir cells and internal wave-driven forcing. With respect to the latter, the work of MacKinnon and Gregg needs to be considered.

AC: As requested we discussed more in detail the role of waves and Langmuir cell in the surface turbulence generation by including an analysis of their role through a regime diagram (new Figure 5). The suggestion on internal waves is interesting, the two intrusions observed during yoyos Y02 and Y03 could develop internal waves but the duration and rate of sampling could not allow for detection of internal waves or for description of their characteristics.

R1C: Abstract, line 9: "ensembles" - not "enables". The need for ensembles is not universal. Just consider the single-cast deep ocean microstructure profiles.

AC: We tend to agree that there is not universal need for ensembles profiles, but in the case of shallow waters and in absence of time and technical constrains, we think that it is appropriate to perform multiple casts in order to obtain more statistically significant observations. The text was modified as suggested.

R1C: Abstract, near Line 15: Attempts at reducing vertical smearing in averages have been done many times before, typically using potential density (or Thorpe-sorted pot. density). This works well in data with vertical displacements due to internal waves. It does not work so well in the presence of lateral water mass variations. I leave it up to the authors to comment on my note or to ignore it.

AC: We accept the idea to comment upon this interesting topic and we we agree with the referee that in case of lateral variation a reduction of vertical smearing could be problematic. In our observations the gap between casts of one ensemble is at most of a 3-5 minutes hence we think that lateral displacements are less likely to occur than vertical ones. Following an observation of referee #3 we moved the description of the algorithm in appendix.

R1C: Introduction, first paragraph: While I agree with the last sentence, the remainder of the opening of the paper is pretty much off the mark. Turbulence observations have become rather common. And from the 1980s microstructure measurements have been accompanied by the necessary ancillary measurements.

AC: Thanks, the paragraph was modified accordingly.

R1C: Page 1734, line 27: What is the "NIB-MBS" profiler?

AC: Two profilers were used during operations, one own by CNR-ISMAR and one by the Marine Station Station of the Slovenian National Institute of Biology (NIB-MBP). This differentiation is now be better explained in text.

R1C: Fig. 3: The red line i (d) is hard to see.

AC: Thanks, the figure was redrawn in higher resolution and with thicker lines. It is now Figure A1 in appendix.

R1C: Fig. 6: As there are only small vertical variations in T, S and turbidity, a set of "waterfall plots" might show more detail of the data. – The contour interval in epsilon obviously is 1 in log(epsilon/(W/kg), not in epsilon itself (ditto in later figures).

*AC: The figure label was adjusted to account for the logarithmic epsilon. We added to figure 6 a waterfall plot (see following figure) but we the result could be misleading. The water column during Y01 was completely mixed with very small vertical variation*confesso che non sono sicuro di cosa vo *of temperature and salinity. In those*

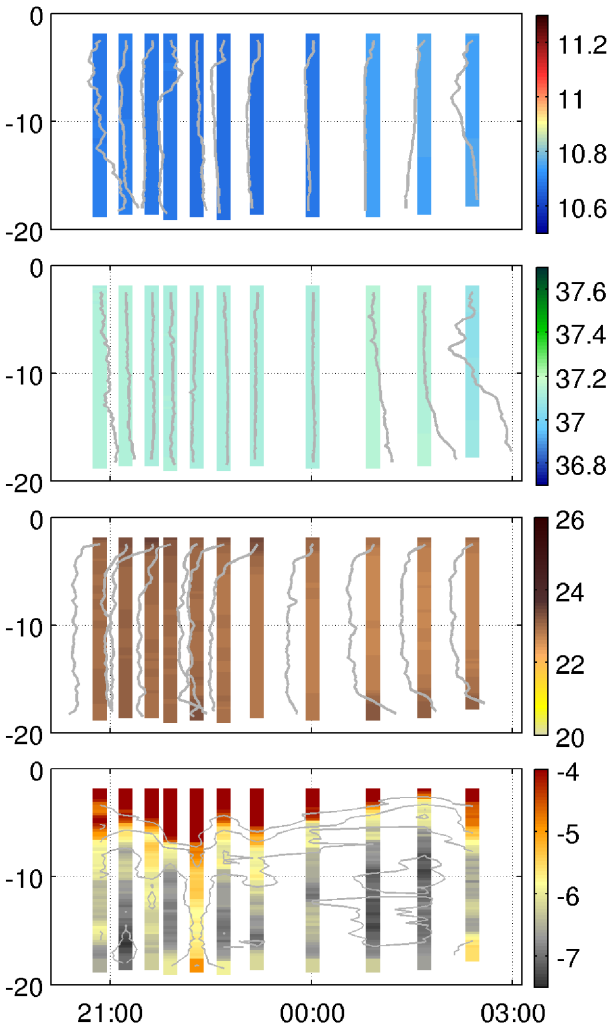

conditions the variability shown by the waterfall could be misleading given that its amplitude is very small.

R1C: Fig. 8: The measured dissipation rates of Yoyo Y01 are described as "in agreement with the local forcing". Yet epsilon is systematically and strongly elevated above the wind-related similarity scaling in the upper 7-9 m. This needs an explanation or modification of the text. The elevated epsilon near the surface is even more pronounced in later Yoyos. See text above for other parts of the data set.

AC: Please refer to the reply to the first comment above.

R1C: Fig. 8: Why not plot the surface buoyancy flux as vertical lines?

AC: we prefer to keep in figure 8 just the scaling, following on the referee comment we added a zoom of the surface buoyancy flux to figures 6 and 9 to be more in line with the text.

Referee #2

R2C: In the manuscript, a detailed and comprehensive analysis of the microstructure observations is presented. It is shown, that the vertical turbulence structure in the water mass is well correlated with the changing forcing and stratification conditions. However, the analysis of the observed TKE dissipation rates with respect to similarity scaling seems me a little bit insufficient. In figure 8 is clearly to be seen, that the dissipation rates in the depth rage below approx. 12m nicely following the similarity scaling, but in the depth rang above 12m the dissipation rates mostly exceeds similarity scaling by 1 to 2 orders of magnitude. Here, a deeper analysis of the measured dissipation rates including effects of wind forcing and surface waves should be carried out.

AC: Thanks for the suggestions, In the revised manuscript we added to section 4 a description of all forcings and of their role in surface turbulence generation. We also remarked that the collected data did not permitted a detailed analysis of the surface TKE.

R2C: 2.1 Meteorological conditions..., page 1735, line 28: cold air mass instead of cold water mass.

AC: Thanks, changed in text.

R2C: The figures are quite small and details are hardly to be seen.

AC: We apologize for this, now most of the figure have been replotted in higher resolution.

Referee #3

R3C: My most relevant concerns, detailed here below, are about the results presentation and the statistical analysis performed. In particular, the paper is somehow difficult to read: the results are worthy to be discussed in a better and clearer way. I find that they are lost among many informations not necessarily relevant, which might be shortened or moved to Appendices. Finally, other corrections are listed at the end of this report.

AC: Following the Referee suggestion the structure of the paper was significantly modified in a more linear way and grammar and syntax were checked (see reply to referee #1). The description of the algorithm using to minimize the smearing effect has been now moved in the appendix. In the Abstract and in Introduction some unimportant details have now been removed.

R3C: 1 The first part of the paper describing the experimental campaign and different features is too long. The reader is sometimes lost in many details, risking to loose the main points of the work. I would ask the authors to make it shorter and less descriptive, but highlighting the main and important features. In the end this is a work about turbulent velocity and velocity gradient measurements, and this should be the focus.

AC: Thanks for the comment: following your indications this part of the paper has been partially reduced. We still think that a detailed description of the atmospheric forcing and of the hydrological conditions is important. Those parts (i.e. sections 2.1 and 2.2) have been kept in a revised form.

R3C: The procedure sketched in Sec. 2.2 is to me justified in its purpose but it is rather arbitrary in the method: I am not sure it significantly improves the data quality. I would ask the authors to move it in the Appendix, together with the associated Figure 3.

AC: The description and Figure 3 have been moved in appendix.

R3C: 2 The turbulent kinetic dissipation rates are extracted from the MSS profilers: we can say that these ARE the most important data in the paper, or among the most important ones. However no detailed info is given on how these are extracted.

Which is the working frequency of the MSS? Which formula is used to derive the TKE from the shear rate measurements? Can the authors show the averaged shear rate spectrum? How is the water column stability accounted for?

AC: We agree with the referee that the TKE observations are the core of the paper but at the same time we believe that it is better not to go too much into detail on the raw data processing, since those aspects are accepted protocols. However, we

added some more informations on the probes and a specific reference that contains all the information on data processing.

R3C: 3 At page 13 of the paper (page 1741), the authors introduce the reference relations they use to estimate the kinetic energy dissipation rates from data. I find that this part of the paper is too vague, in particular since the focus of the work is turbulence. First the authors should cite the literature they refer to in this sentence:

***"It is generally accepted that mechanical generation of turbulence due to surface wind stress (εs) follows a law of the wall relationship for which[...]"*.**

Second and most importantly the authors should explain exactly how and where they use Eq. 2. How is the surface wind stress *τa* estimated? Which value is used for *z*? Are there any corrections due to drag coefficients? and if yes which ones? Also, with MSS, TKE can be extracted from scalars behaviour. It would be interesting to check how TKE derived from the shear rates compare to that extracted from scalars microstructure.

AC: In the revised paper a specific section (3. Turbulence scaling) was added to address these observations. The scaling approach has been better explained and the relevant literature cited. As stated in the text the *τa* is computed from atmospheric data using the COARE algorithm.

While it is possible to extract TKE from MSS, that is outside the scope of the present study. We will try do expand this in a following paper and we thank the reviewer for pointing out.

R3C: 4 Still at page 13 and then 14 (1741 and 1742), the authors refer to the turbulent kinetic energy dissipation rate *εsb* due bottom shear stress, estimated from the bottom friction velocity *εu∗b*. Observations similar to those expressed above arise for the application of eqs. (4) and (5). As the authors clearly state *Hence the bottom stress computed using a drag coefficient of 0.003 and quadratic drag law needs to be regarded as just a rough estimation.* Why have the authors not used ADCP data to extract an alternative "estimate" of ε_{sb}? The first one is by using the turbulent kinetic energy spectrum: although the ADCP frequency is moderate, an attempt could be done. The second one is by using the ADCP data to estimate horizontal velocity vertical gradients in terms of velocity increments along the vertical direction, and then applying $Cv(\partial u/\partial z)^2$, where *C* is an order one constant. Again, since the focus of the paper is turbulence measurements, the authors should pay more attention to this part.

AC: We agree that it would have been very interesting to try this approach in our data analysis. Unfortunately the ADCP data collected during CARPET2014 were recorded with an instrument mounted on the R/V hull about 4 m below sea surface, with a 4 m thick recording bin and with the first bin centred at 7.5 m. Given an average depth of 20 m, the acceptable observations inside the GoT were at most 3 points in each water column. Hence, observations collected are not enough to have a good computation of current shear. This approach have been tried before in the Adriatic

Sea (Carniel et al., "Turbulence variability in the upper layers of the Southern Adriatic Sea under a variety of atmospheric forcing conditions", Continental Shelf Research, 44(2012)) but with higher vertical resolution and deeper water column.

recorded observations in cells of 4 m. This with the loss of the the first few meters (the ADCP was mounted). that, for any given point inside the GoT, results in 3 to 4 observation in the water column, that does not permit a computation of horizontal shear at the necessary resolution.

R3C: 5 I would ask the authors to rephrase the Conclusions. While a short summary of the content of the paper is useful, a long discussion is not needed. To me, the main point of the paper is that TKE measurements are highly variable (as it is known in turbulence in general), and can be influenced by different features in ocean turbulent flows, in particular. Density stratification and the impact of suspended sediments have to be better investigated to be able to quantify, at least phenomenologically, ranges of values for which TKE is substantially modified.

AC: We followed the suggestion of Referee #3 and now summary and discussion sections have been merged and shortened. In order to highlight the most important findings these have been synthesized in a bulleted list.

Other corrections:

1 at Page 1739, it is written *Shear data from both profilers were used to determine the turbulent kinetic energy dissipation rate (ε), the dissipation rate of temperature variance (χ), eddy (K_ρ) and heat diffusivity (K_h) and the Thorpe scale (L_T).* Where are these data discussed? Am I missing something?

AC: All references to parameters that are not discussed in the paper have been removed.

R3C: 2 page 1741, line 15 : ε_b is to be replaced by ε_{sb} and ε_{u*a} is to be replaced by ε_{u*b}.

AC: Thanks, text have been corrected accrdingly

R3C:3 Caption of Figure 1: fro –¿ for; insert –¿ inset.

AC: Thanks, the caption for Figure 1 was corrected.

R3C: 4 The list of Reference is to me a bit unbalanced. Authors refer to lots of papers about the Adriatic circulation, but references about turbulence analysis are unexplainably missing.

AC:Thanks, the reference list was updated and integrated.

Major changes in the revised manuscript:

- The structure of the paper was modified :

  Abstract

  1.Introduction

  2. Observations and data processing

    2.1 Meteorological conditions and surface forcing

    2.2 Hydrological conditions and water mass structured

  3. Turbulence scaling

  4. Yoyo coasts and turbulence observations

  5. Summary and discussion

  Appendix A

- The abstract was modified and shortened;
- In the Introduction unnecessary details were removed;
- the description of the algorithm used to minimize the smearing effect is now in appendix;
- a new section was introduced specifically for turbulence scaling;
- the data collected by the WASS stereo system are described and integrated in the manuscript;
- a regime diagram (figure 5) was produced to explain the role of surface forcing;
- the summary and discussion section has been shortened and results have been summarized in a bulleted list;
- most figures have been improved:
  - Figure 2: the Stokes drift has been added to panel d and the labels have been corrected;
  - Figure 4: labels are in bigger font and data are plotted with bigger dots;
  - Figure 5: not present in the first manuscript;
  - Figure 6: panel a was added to show wind stress and buoyancy flux;
  - Figure 8: thicker lines are now plotted
  - Figure 9: panel a was added to show wind stress and buoyancy flux;
  - Figure A1: thicker lines are now plotted

Turbulence observations in the Gulf of Trieste under moderate wind forcing and different water column stratification

F.M. Falcieri[1], L.Kantha[1,2], A. Benetazzo[1], A. Bergamasco[1], D. Bonaldo[1], F. Barbariol[1], V. Malačič[3], M. S. Sclavo[1], S.Carniel[1]

[1]{Istituto di Scienze Marine – Consiglio Nazionale delle Ricerche, Venezia, Italy}

[2]{Colorado Center for Astrodynamical Research – University of Colorado, Boulder, CO, USA}

[3] {National Institute of Biology, Marine Biology Station, Piran, Slovenia}

Correspondence to: F. M. Falcieri (francesco.falcieri@ve.ismar.cnr.it)

Abstract

During tThe oceanographic campaign CARPET2014, between (January 30th - and February 4th 2014), collected the very first turbulence data in the Gulf of Trieste (Northern Adriatic Sea) under moderate wind (average wind speed 10 m s^{-1}) and heat flux (net negative heat flux ranging from 150 to 400 W m^{-2}). Observation consisted of 38 CTD casts anda total of 478 microstructure profiles (grouped into 145 ensembles) with three sets of yoyo casts, each lasting for about 12 consecutive hours. Overall, these represent the first turbulence observations collected in the Gulf of TriesteAmong the collected profiles, there were three sets of yoyo casts, each lasting for about 12 hours for a total of 50 casts. 150 to 400 W m^{-2}). in the range of in the Gulf of Trieste (Northern Adriatic Sea) under moderate wind forcing (average wind speed 10 m s^{-1}) and heat fluxes (net negative heat flux madewere and 38 CTD casts .Averaging closely repeated casts, such as the ensembles, can lead to a smearing effect when in the presence of a vertical density structure with strong interfaces that can move up or down between subsequent casts under the influence of tides and internal waves. In order to minimize the smearing effect of such displacements on mean quantities, we developed an algorithm to realign successive microstructure

profiles to produce sharper and more meaningful mean profiles of measured turbulence parameters.

~~Microstructure profiles collected with a free-falling profiler must be taken in enables of repeated casts, with the objective of obtaining more statistically significant values for turbulence parameters. This approach is certainly feasible in shallow waters, but has a down side when the vertical density structure includes strong interfaces that can move up or down between subsequent casts, under the influence of tides and internal waves. In order to minimize the smearing effect of such interfacial displacements on mean quantities, we developed an algorithm to realign, according to the temperature profile, successive microstructure profiles to produce sharper and more meaningful mean profiles of measured turbulence parameters.~~ During ~~CARPET2014~~the campaign, the water column in the Gulf evolved from ~~a~~ well-mixed ~~condition~~ to ~~a~~ stratified conditions due to Adriatic waters intruding at the bottom along the Gulf's south-eastern coast. ~~In this study, w, which in turn stability characteristicsitschanged stratified the water column and These waters~~ We show that during the~~a~~ warm and relatively dry winter~~, such as in 2014,~~ the water column in the Gulf of Trieste~~, even under moderate wind forcing,~~ was not completely mixed ~~because~~due to ~~of~~ the influence of bottom waters intruding from the open sea~~, even under moderate wind forcing~~. Inside the Gulf, two types of water intrusions ~~from the Adriatic Sea~~ were ~~observed~~found during ~~the~~yoyo casts: one coming from ~~its~~the Adriatic Sea northern coast (i.e. warmer, saltier and more turbid) and one coming from the open sea in front of the Po Delta (i.e. cooler, fresher and less turbid). ~~Those~~The two intrusions ~~behaved similarly but~~ had ~~a~~ different impacts on turbulence kinetic energy dissipation rate profiles. The former, with high turbidity, acted as a barrier to wind-driven turbulence, while the latter, with low sediment concentrations and a smaller vertical density gradient ~~when compared to the rest of the water column~~, was not able to suppress downward penetration of turbulence from the surface~~. to the same degree.~~

1 Introduction

Turbulence~~In recent years, turbulence~~ and associated processes ~~have~~are gain~~ing~~ed a broader interest within the ocean sciences community for their fundamental role in many ocean phenomena (Garget, 1997; Thorpe, 200~~4~~5). Because of their

importance in issues such as ocean mixing, energy transfer, dissipation or dispersion of nutrients and pollutants, a better understanding of turbulent processes is paramount for ocean sciences. ~~Yet, direct turbulence measurements in the ocean are still scarce and are not routinely performed. Moreover, when made, these observations are generally not accompanied by auxiliary measurements (such as surface winds, waves and currents) necessary for their interpretation.~~ While turbulence observations have become more common in recent years there ~~hereT~~ is ~~therefore~~still a need to collect more ~~complete~~ datasets ~~suitable~~ for use in the analysis of mixing in the water column, and to improve ~~the~~ turbulent mixing parametrization~~parameterization~~ in numerical ocean models (Carniel et al., 2012).~~The Adriatic Sea is an elongated basin (800 km long and 200 km wide, Figure 1) located in the northernmost part of the Mediterranean Sea. It presents a wide but shallow shelf area (200 km x 200 km and 35 m of average depth) generally referred to as the Gulf of Venice, the first shallow pit system in its central area with the two Pomo depressions with a maximum depth of 260 m and the Southern Adriatic Pit (SAP) that reaches depths up to 1200 m. The water budget is mostly defined by fluxes across the Otranto strait and by inputs of the Po (north-western coast) and Albanian rivers (south-eastern coast) that have significant seasonal variations (Csanady, 1982, Raicich M., 1996). Atmospheric forcing is strongly influenced by the surrounding land topography, more specifically by the jets of the Bora (a strong seasonal katabatic wind) blowing across the Adriatic Sea from north-east and the Scirocco wind blowing from the south east along the basin main axis (Malačič et al., 1999).~~

The Gulf of Trieste (GoT henceforth) is a small and shallow bay (maximum depth less than 30 m) located in the northeastern corner of the Adriatic Sea (Figure 1). It is generally classified as a region of freshwater influence (ROFI, Simpson, 1993~~7~~) due to intense riverine discharges and undergoes~~, with~~ a marked seasonal variability. The GoT hydrodynamics are driven by~~that strongly influences the general circulation. The second driver of the hydrodynamics of the GoT is~~ winds (Bora and S~~c~~irocco), tides, ~~and~~ buoyancy effects of the Isonzo ~~river~~River plume and exchanges of water masses with the Adriatic Sea. The north-easterly Bora ~~winds~~ generates a cyclonic circulation in the N~~n~~orthern Adriatic and pushes surface waters out of the GoT, inducing a compensating inflow of open sea waters near the bottom (Malačič et al., 2012). The

inflow/outflow transport is governed by topographic control of the wind-driven circulation (Csanady, 1982). During Sirocco winds however, the water masses at the surface are driven to the northern shore of the Adriatic Sea between Venice and Trieste, where they bifurcate in front of the GoT. The eastern sidepart of the flow turns right and enters the GoT along its northern coastline, while the western partside turns left and contributes to the coastal current flowing towards the Venice lagoon. (Malačič et al., 2012).

The Isonzo riverRiver plume, during windless conditions, occupies the surface of the northern GoT with inertial motions near the river outlet, while along the frontal line that embraces the plume's bulge there is resulting in a quasi-geostrophic motion andwith a convergence zone along the frontal line that embraces the plume's bulge (Malačič et al., 19969). Due to vertical mixing of the surface fresh water with sea water across the halocline, this plume induces thean inflow of water masses near the bottom of the GoT (Malačič and Petelin, 2001). The Isonzo plume and its variability play a fundamental role in driving the bottom circulation of the GoT. The annual mean flow rate of the Isonzo River was aboutbetween 1998-2005 was around 90 m^3 s^{-1} from 1998 to 2005 (Comici and Bussani, 2007), but different estimates, varying by a factor of three from this value, can also be found in literature. In January-February, the monthly mean flow rate 1998-2005 inranged from 1 m^3 s^{-1} to 351 m^3 s^{-1}, with 41 m^3 s^{-1} on the average (Comici and Bussani, 2007) during the 1998-2005 period. In 2014, the Isonzo riverRiver experienced a period of strong discharges, with February 2014 average discharge rising to 547 m^3 s^{-1}. During the sampling period inside the GoT, the mean discharge was 868 m^3 s^{-1} with maximum and minimum values of 1768 m^3 s^{-1} and 327 m^3 s^{-1} respectively (according to data collected from the hydro-meteorological service of Friuli Venezia Giulia, *"Servizio Idrometeoreologico – Protezione Civile Friuli Venezia Giulia")*. This unusually large discharge rates have an effect on the surface denisty structure, which in turn affects near-surface turbulence characteristics.

Turbulence measurements in the Adriatic Sea are scarce and scattered. By far, the largest number of available casts is retained by the "Istituto di Science Marine – Consiglio Nazionale delle Ricerche " (CNR-ISMAR), with more than a thousand quality-controlled samples, ranging from a few meters to over 900 meters in depth. To

our knowledge, a very limited number of papers dealing with this topic have been published in literature. Peters and Orlić (2005) presented the first measurements of turbulence in the Adriatic Sea with a set of 32 casts in the central basin collected in May 2003 within the framework of the DOLCEVITA project. During the collection period, wind forcing was weak and the water column generally well stratified with a shallow mixed layer depth. The authors found small values for the turbulent kinetic energy (TKE) dissipation rates in the upper mixed layer. Peters et al. (2007) reported a second set, collected in February 2003 also within the DOLCEVITA project in the shallow northern Adriatic under strong winds, intense cooling and a well-mixed water column. ~~Their data consist of seven microstructure stations and two deployments of a bottom lander with an upward looking ADCP.~~ Their main findings highlight different contributions of surface forcing and bottom friction on the TKE dissipation rate profiles. At both study sites, the main contribution to turbulence generation was found to be mechanical ~~rather than~~and buoyancy effects were small.

Carniel et al. (2008) discussed two sets of repeated observations ~~(for a total of 47 casts)~~ in the southern Adriatic Sea in front of the Gargano peninsula during the March 2006 DART06A cruise. Their ~~microstructure~~ studyies revealed layered thermohaline staircase structures that originated from double diffusive convection. During the DART06B cruise (August 2006), Carniel et al. (2012) collected ~~the most comprehensive turbulence data set published to date for the Adriatic Sea. A~~ a total of more than 300 casts, which allowed them~~the authors~~ to describe the upper oceanic mixed layer under a series of different meteorological conditions (different wind forcing, night-time convection and strong insolation). ~~A set of microstructure observations with a free-falling probe has been collected in June 1990 by J. Imberger with the support of Marine Biology Station (NIB-MBS) in Piran, but at the time of publication of this article that data set is still unpublished.~~

All of the studies cited above deal almost exclusively with the surface mixed layer and only in Peters et al., (2007) there is a discussion of the role of the bottom boundary on turbulent dissipation rates. This means that the interaction between surface and bottom turbulence has only been described briefly in the Adriatic Sea. ~~However, two recent sets of observations deal with the role of the sea floor and its influence on turbulence and sediment transport. The first set (currently under~~

~~publication) was collected over a field of mud waves in spring 2013 in southern Adriatic during the DECALOGO2013 campaign on board R/V *Urania*. During the cruise, TKE dissipation rates were documented in four transects over a field of mud waves located in the Southern Adriatic Shelf edge, an area that is influenced by the Northern Adriatic Dense Water.~~

In this study will be described a sub-set of ~~In this paper, the observational data~~observations collected during ~~from~~ the CARPET2014 campaign ~~will be described. Operations~~ on-board the R/V *Urania* in the northern Adriatic Sea between the 29th of January and the 10th of February ~~will be described~~.

2 ~~Measurements~~Observations and data processing

The CARPET2014~~turbulence~~ data set (Benetazzo et al., 2015) was collected ~~in the winter of~~ between January 30th and February 10th 2014 in the ~~GoT and in front of the Po river Delta~~Northern Adriatic Sea. In this work only the data collected inside the GoT will be discussed (Figure 1). ~~using two microstructure (MSS) profilers. Apart from~~

Turbulence measurements were made with two microstructure profilers (MSS 90, Prandke et al., 2000)~~Each cast was made by dropping the MSS profiler~~ allowed to ~~in~~ free fall until they hit the sea floor~~and recording physical parameters until the probe the sea floor~~. This operational procedure permitted collection of observations very close (8 cm from the bottom) to the sea floor. During the cruise, 818 casts were ~~collected~~made at 104 stations, 554 with a MSS profiler owned by ISMAR-CNR and 264 with ~~the~~ one owned by the Slovenian National Institute of Biology (NIB-MBP) ~~profilerS~~. At each station, three to five profiles were measured, which were then ~~casts wereof each station's all~~ averaged to obtain a mean profile representative of the water column ~~condition~~ during sampling. We will refer to these profiles as ensemble casts.

Among all the stations, three~~3~~ were in yoyo mode~~. By yoyo mode, we mean~~, i.e. a series of repeated casts in a fixed location with the R/V either at anchor or ~~dynamically~~ keeping the position dynamically. A yoyo series is helpful in studying the temporal evolution of the water column at a ~~fixed~~given location, but at the loss of synoptic and spatial information. ~~A subset of the collected observations will be used in this paper, more specifically the casts collected inside the GoT between January~~

~~30th and February 4th.~~ The three yoyo casts (Y01, Y02 and Y03) were made at two ~~locations~~stations close to each other in the deepest part of the GoT (blue squares in right panel of Figure 1) with a sampling rate of 30 minutes (~~each set~~ specifics of each set~~specifcs~~ are reported in T~~t~~able 1~~2~~). During the last part of Y03, the sampling ~~frequency~~rate was increased to every 15 minutes.

The temperature and salinity measurements from the two MSS probes were calibrated against CTD observations by pairing the first cast of each MSS ensemble to its spatially and temporally closest CTD. Of all possible pairings, only those that were closer than 1000 m and taken less than 15 minutes apart were considered. In order to have an optimal cross calibration, all profiles with a stratified water column were ignored (i.e. those profiles that presented a salinity range higher than 0.3 ~~PSU~~ or a temperature range higher than 0.5 °C). This was necessary because in the presence of a thermocline or halocline, even a small vertical displacement (due to interface oscillations) between casts could result in measures of different values at the same depths and hence errors in calibration.

The bias, root mean squared error (RMSE) and percentage root mean squared error (PRMSE) of each pair were computed, and all profiles with PRMSE less than 1% were used to compute each sensor bias. Results are shown in Table 2~~1~~.

Among all the profiles collected by the ISMAR probe, 73 pairs ~~were identified following~~satisfied the spatial and temporal proximity criteria and 21 were selected for cross calibration based on vertical stratification criterion. The NIB probe had 60 pairs, with ~~and~~ 28 of those eligible for calibration. For all profiles the BIAS and RMSE are very low, almost at the precision limit of each sensor, and PRMSE values are therefore small. The only sensor that shows a significant BIAS (-0.2418 ~~PSU~~) is the salinity sensor on the ISMAR profiler, which was therefore corrected for later computations.

The two microstructure profilers acquired data at 512 Hz to allow collectionof observation every 0.0011 m (given an average fall speed of 0.6 m s^{-1}). Both probes were equipped with standard CTD sensor (pressure, temperature and conductivity) and two shear sensor and a fast temperature for the water column microstructure. Shear data from both profilers were used to determine the turbulent kinetic energy dissipation rate using (Gregg, 1987; Peters 2007)

$$\epsilon = 7.5\,\nu\left(\frac{du}{dz}\right)^2 \qquad (1)$$

where *du/dz* is the velocity shear and *v* is the kinematic viscosity. Details of the protocol used for data processing can be found in Prandke et al. (1998); the algorithm used to minimize the smearing effect of interface observations are given in Appendix A.

In addition to the microstructure profiles ~~described below~~, ancillary observations include 104 CTD casts with SBE 911, current measurements ~~were~~ made with a downward looking hull-mounted ADCP (RDI workhorse 75 KHhz, acoustic bin size set to 4 m with a blank interval of 5 m and first bin centred at 7 m), and meteorological forcing ~~was~~ acquired by the R/V *Urania* ~~*hull-borne*~~ weather station and by the ~~NIB~~ Slovenian coastal observatory VIDA~~buoy~~. During selected periods 3D sea surface wave field measurements were made with a Wave Acquisition Stereo System (WASS, Benetazzo et al, 2012) mounted on the port side of the R/V bridge about 8 m above the mean sea level.

2.1 Meteorological conditions and surface forcing

~~Winter 2013-2014, c~~Compared to the climatological mean, the winter of 2013-2014 can be considered ~~to be~~ dry and warm ~~and wind light rain with~~. ~~But,~~with January 2014 and the period of the CARPET2014 cruise were anomalously warm and moist. During the campaign, ~~there was~~ a warm and moist air mass was flowing from the southeast (northern ~~coastline of~~ African coast) over the northern Adriatic region ~~while~~and ~~Dinaric mountain ridge that constitutes the northeastern corner of the Adriatic Sea.~~, aAt the same time, a cold ~~water~~air mass was flowing from the eastern part of the European continent towards the northern Adriatic Sea. ~~A strong temperature inversion was present at around 1000 m altitude, where over a thickness depth of 400 m, the air temperature increase with height was 8 °C, as revealed by a balloon sounding over Ljubljana in the early morning of 2nd February 2014 [Sinjur et al., 2014]. In the northeastern landscape of the Adriatic Sea, this weather constituted an extreme sleet hazard in Slovenia, which was struck by a severe ice storm.~~

Atmospheric data, sea surface temperature and salinity ~~(Figure 2, left panel)~~ were recorded throughout the cruise ~~from~~by the R/V *Urania*'s ship-borne weather station

(located about 10 m above sea level) and by a thermistor and a salinometer mounted on the R/V hull, about 2 meters below sea level (Figure 2, left panel). The latter~~,~~ ~~when compared to CTD data, presents~~ had a bias of 0.2 ~~psu~~ when compared to CTD data~~,~~ and hence its measurements used for computation of fluxes~~,~~ were corrected accordingly~~for bias~~. The R/V *Urania* sailed in the GoT and did not hold a fixed position, and therefore, in order to have a complete representation of the atmospheric conditions, the ship-borne weather observations need to be supplemented by a fixed observation point. Data collected from the Slovenian coastal observatory VIDA were ~~then~~ also used for computation of fluxes (Figure 2, right panel). The VIDA buoy is anchored at a depth of 22 m about 2.3 km off the coast in front of Piran (https://www.nib.sl/mpb/en/buoyancy/general). Atmospheric observations and fluxes computed using the two datasets showare ~~strongly~~ similarityence ~~H.~~, and therefore their merged analysis can be considered to be ~~as~~ representative of the atmospheric conditions over the whole GoT during the campaign. The small scale variations in R/V *Urania*'s dataset can~~have to~~ be ascribed to a higher sampling rate (one record per minute) with averaged~~d~~ over 10 minute intervals used for flux computations, compared to the 30 minute averages ~~of~~for the VIDA buoy dataset.

~~Wind observations taken from R/V *Urania* and at *VIDA* buoy are very similar (Figure 2, panel b).~~ At the beginning of observations~~the measurements~~, easterly Bora was turning to a south-east S~~c~~irocco (~~about~~ ~10 m s^{-1}) that lasted for two days until the night of February 2nd, when it turned back to Bora with an average wind speed~~s~~ of~~above~~ 10 m s^{-1} with peaks of 16 m s^{-1} (Figure 2, panel b);~~.~~ d~~D~~uring the S~~c~~irocco event, three calm periods were recorded with weak winds from north. Air temperature showed~~sshow~~ a similar pattern with lower values during Bora (between 5 and 8 °C) and~~,~~ a warmer one during S~~c~~irocco (up to 14.5°C). The three calm periods can also be seen in air temperature, with sudden drops of about 5 °C. Throughout the cruise, sea surface temperature was rather constant around 11.5 °C with an increasing trend toward the end of the operations (Figure 2, panel a). The ship-borne observations showed a stronger variability with respect to the VIDA ones due to the R/V positional changes within the GoT. Analogous behaviour was also~~can be~~ seen in sea surface salinity (not shown).

Figure 2 ~~(panel c)~~ shows also the heat fluxes (panel c) and wind stress (panel d in cyan) computed using the COARE algorithm (Fairall et al., 2003), from on site-observations (sea surface temperature and salinity, air temperature, pressure and humidity) and from short and long wave radiation. The radiation fields ~~are~~were derived from an implementation of the Coupled Ocean Wave and Sediments model over ~~C~~centrale Europe with a 7 km horizontal resolution (Ricchi et al., 2015, under review).

~~N~~The net heat flux ~~is~~was always negative at both sites, with a heat loss from the ocean to the atmosphere always higher than 150 W m^{-2} during Bora events (peaks of just over 400 W m^{-2} at *Urania* and 350 W m^{-2} at *VIDA*). During S~~c~~irocco events, fluxes were generally smaller, with heat losses ~~in the range of~~of around 100 W m^{-2}. It is noteworthy that on the one hand the latent heat flux ~~is~~was always negative, but on the other hand, sensible heat flux turned~~s~~ positive during S~~c~~irocco due to air temperature being higher than the sea surface temperature. ~~not the case is~~This Duringuring~~d~~ the three calm periods, ~~when~~ a drop in wind speed and air temperature, below the sea surface temperature, resulted in a switch in the sensible heat flux direction.

The buoyancy flux at the surface (Figure 2 panel d) was obtained following Shay and Gregg (1984~~6~~, 1986~~4~~) as:

$$J_b = \frac{g}{\rho_w}\left(\frac{\alpha}{C_p}J_t + \frac{BS}{L_E(1-S)}J_l\right) \qquad (~~1~~2)$$

in which the first term inside brackets represents the heat buoyancy flux, computed from the net heat flux (J_t), the thermal expansion coefficient (α = -2.16 x 10^{-4}~~3~~ $°C^{-1}$) and the sea water specific heat (C_p = 3.98 x 10^{-4} K^{-1}), while the second term ~~one shows~~is the evaporative buoyancy flux computed from the latent heat flux (J_l), the haline contraction coefficient (β = 0.79), the latent heat of evaporation (L_E = 2.6 x 106 J Kg^{-1}) and sea surface salinity expressed as concentration. The convention used for heat and buoyancy fluxes in this study is that negative/positive fluxes correspond to losses/gains from/to the ocean to/from the atmosphere. In the case of buoyancy, this means that a negative J_b corresponds to a loss of buoyancy from the ocean to the atmosphere (i.e. water is getting less dense) with a stabilizing effect on the water

column, while positive J_b indicates a gain of buoyancy (i.e. water becoming ~~less~~more dense) and hence a destabilizing effect on the water column.

2.2 Hydrological conditions and water mass structure

~~During the sampling period, the GoT was subject to moderate wind forcing, with an average wind of over 10 m s^{-1} and peaks of 16 m s^{-1}, starting with Scirocco from January 30th to February 1st and then Bora winds. During the first fase, two calm wind periods with velocities below 2 m s^{-1} can be observed (Figure 2).~~ The hydrological conditions in the GoT during CARPET2014 are the result of the forcing described in section 2.1,~~this type of forcing on the GoT is~~ a combination of wind-driven circulation during the two prevalent winds (Bora and Sirocco)~~(as pointed out in the introduction)~~, with inertial oscillations in offshore areas~~where those winds prevail,~~ during times of wind shifts from ~~the~~ one type to another and during periods of calms between windy episodes.

Weather and ship logistical constraints did not permit a synoptic hydrological survey of the entire GoT, hence~~. Instead,~~ different parts of the basin were covered each day. In order to give a rough overview of the hydrodynamics of the GoT, surface (from 0 m to 2.5 m) and bottom (last 2.5 m of cast) temperature and salinities collected on January 30th and 31st, and February 4th from CTD casts are shown in Figure 34 along with the bottom currents measured by the hull-mounted ADCP.

The overall picture that emergi~~es~~ng from Figure 34 is a bottom circulation with waters incoming from the open sea along the southeastern coast and flowing out along the northwestern one (left panels). The same pattern is common to both tidal intervals, during rising (red arrows in Figure 34 left panels) and falling (blue arrows in Figure 34, left panels) tides, with the latter showing weaker currents. The intervals of rising and falling tides have been defined from the pressure values recorded by the bottom mounted ADCP located at the VIDA buoy. The apparently incoherent vectors close to the coast can be explained by the influence of the coastline and of the shallow topography on the local currents. Each plot shows a 24h collection of data over a relatively small area, and ~~hence can~~may also include small-scale variations.

Temperature and salinity distributions (Figure 34) are in agreement with the general picture of warmer and saltier bottom waters entering the southern part of the GoT and cooler and fresher waters confined ~~in~~to the northern part. The low surface salinity

values in the northernmost part and in front of Trieste (Figure ~~4~~3, right panels) are the result of the influence of the Isonzo and Timavo discharges (Figure 1, left panel), respectively. It is of interest ~~to note~~ that on February 4th, the easternmost stations ~~are~~were warmer and saltier throughout the water column than those on January 30th. This cooling of the water column ~~is~~was due to the ~~constant~~steady negative heat flux between Y02 and Y03 (Figure 2).

The θ-S (potential temperature – salinity) plot (Figure 4), computed from both CTD and MSS data, ~~in Figure 5~~ helps in the identification of the water masses that were present in the GoT and in the Northern Adriatic Sea during the ~~operations~~campaign ~~from the CTD and MSS surveys~~. Inside the GoT (dark grey dots in Figure ~~4~~5), the water temperature was lower than ~~that~~that ~~in the~~ outside of the basin (light grey dots in Figure ~~4~~5), due to the moderate negative net heat flux throughout the cruise (ranging between -150 to -400 W m^{-2}) and the shallow bathymetry of the GoT. Apart from the Isonzo ~~river~~River mouth and the inner part of the Gulf, salinity ~~s~~show values comparable to (or ~~just short of~~ slightly smaller than) the rest of the Adriatic Sea. By looking at Y02 and Y03 casts (red and green dots ~~in Figure 5~~), it is possible to highlight the different origins of part of their ~~the~~ bottom waters. More specifically, ~~yoyo series~~ Y02 presents deep waters (dark green in the left panel of Figure ~~4~~5l) whose θ-S values are directed towards an end point (green circle in the left panel of Figure ~~4~~5, location shown in Figure 1, right panel) close to the density isoline 1029 kg m^{-3}~~-3~~, compatible with Northern Adriatic coastal waters (i.e. fresher, cooler and more turbid waters~~, Figure 5, right panel) (~~ observed right outside the GoT on January 30th ~~typical of Northern Adriatic coastal waters~~. On the other hand, yoyo 03 (Y03) θ-S values of bottom waters have an end-point (red circle in left panel of Figure ~~4~~5, location shown in Figure 1 right panel) typical of the open basin, slightly warmer, saltier and cleaner waters (Figure ~~4~~5, right panel). Moreover, in the case of Y03 end-point, its characteristics are similar to the open sea bottom waters in front of the Po Delta (black rectangle in the left panel~~Figure 5, left pane black square~~) during periods of low discharges (Falcieri et al., 2013). The slight misalignment of those θ-S points with respect to the Y03 endpoint can be explained by their position being still close to the influence of the Po ~~river~~River plume. Both end points are located over the same station but were recorded four days apart, the first one on January 31st and the second one on February 4th.

The wave field over the GoT was assessed from data collected by the WASS system on the R/V and at the VIDA buoy. A total four WASS acquisitions, each of roughly 15 minutes, were collected between 12:05 UTC and 14:32 UTC of February 3rd, right before Y03, and resulted in average significant wave height (*Hs*) of 0.8 m, period (*Tm*) of 3.9 seconds and wave length of 23 m. During the acquisition the wind forcing was stable, with a mean wind speed of 14 m s^{-1} and direction of about 75°N (typical of Bora wind).

To cover a longer part of the study period, the wave and wind data collected at the Vida buoy were used. The wave spectrum *E(f)* of each sea state at the buoy was represented by the JONSWAP spectrum (Hasselmann, 1973). This assumption is consistent with the spectrum computed from the R/V with the WASS observations. A further verification of this is that the *Hs* and *Tm* computed at VIDA with JONSWAP (given the wind speed and fetch length) are close to those directly observed. This spectrum, which models the distribution of wave energy in deep water fetch-limited sea states, was used to compute the Stokes drift (*Us*) following Hasselman (1970) as

$$\vec{Us}(z)=\int_0^{\infty}\frac{1}{g}(2\pi f)^3 E(f)\exp\left(-\frac{2}{g}(2\pi f)^2 z\right)\vec{k}\,df \qquad (3)$$

where *z* is the vertical coordinate positive upwards, *g* the gravitational acceleration, *f* is the frequency in Hz and *k* is the unit vector in the wave propagation direction. During the period under investigation, fetch-limited and deep-water conditions occurred from February 2nd, 2014, 00.00 UTC to February 4th, 2014 12.00 UTC, as moderate and persistent Bora winds were blowing over the Gulf of Trieste (Figure 2). A further verification of this approach is given by the fact that the Stokes drift computed from the WASS spectrum (0.06 m s^{-1}) is in good agreement with the value computed at VIDA (0.05 m s^{-1}). The *Us* time series (dark green line in figure 2 panel d, right side) closely follows the wind stress with values ranging from 0.01 m s^{-1} to 0.07 m s^{-1}.

3 Turbulence scaling

Ocean turbulence is generated and enhanced by different processes such as the shear stress at the sea surface or the bottom, buoyancy fluxes and unstable stratification, breaking and motion of surface and internal waves and wave-current

interactions (Burchard et al., 2008, Thorpe, 2005, Kantha and Clayson, 2004). In this study the observed TKE dissipation rate profiles will be compared to their forcing with a similarity scaling approach (Peters et al., 2007) to highlight discrepancies between the theoretical and the observed profiles, identify the dominant forcing and show the role of buoyancy interfaces in suppressing turbulence in the water column.

Turbulence generated by surface wind stress obeys a law of the wall scaling below the wave-influenced surface region (D'Asaro et al., 2014, Thorpe, 2005) as

$$\epsilon_s = \frac{u_*^3}{k\,|z|} \qquad (4)$$

where $k = 0.4$ is the von Kàrmàn constant, z is the distance from the sea surface and u_{*a} is the friction velocity given by

$$u_* = \left(\frac{\tau_a}{\rho}\right)^{1/2} \qquad (5)$$

in which τ_a is the wind stress computed with the COARE algorithm from wind speed at 10 meters height and ρ is the surface water density computed from the R/V's hull-mounted instruments. This scaling is valid for the surface layer either under calm sea conditions or below a depth at which turbulence generation by wave breaking or wave-current interactions becomes insignificant (Burchard et al., 2008,, Thorpe, 2005).

The law of the wall approach is valid also for turbulence generated by bottom shear stress above a few centimetres thick viscous layer. As for the wind stress generated turbulence, the TKE dissipation rate near the sea floor can be scaled as:

$$\epsilon_b = \frac{u_{*\mathrm{b}}^3}{k\,|h|} \qquad (6)$$

where h is the distance from the sea floor and u_{*b} the bottom friction velocity given by

$$u_{*\mathrm{b}} = \left(\frac{\tau_b}{\rho}\right)^{1/2} \qquad (7)$$

in which the bottom shear stress (τ_{*b}) is computed with a non linear function of the depth averaged velocity with a quadratic bottom drag law computed as

$$\tau_b = \rho C_D u^2 \qquad (8)$$

where ρ is the local water density, u the average bottom current speed as recorded by the downward looking ADCP and $C_D = 0.003$ is the bottom drag coefficient (Peters et al., 2007). In the case of Y02 and Y03, current observations are the average of the cell that span from 13 to 17 m depth, roughly 8 m above the sea floor. Hence the bottom stress here computed needs to be regarded as just a rough estimation.

It is common to assume that the dissipation rate due to buoyancy in the surface mixed layer is uniform and equal to $\varepsilon_b = cJ_b$. The value of the constant c is trivial to define and different figures have been proposed ranging from $c = 0.25$ for the surface upper bound and $c = 0.4$ under strong pycnoclines (Kantha, 1980) to $c = 0.6$ (Shay and Gregg 1986, Peters et al. 1988). Here the latter parametrization will be used.

The wave contribution to turbulence in the surface layer is a more complex topic since it consists of three different processes: wave breaking, Stokes production and the development of Langmuir circulation. In the case of wave breaking, the contribution to TKE is generally confined to a depth of the order of the significant wave height and is dissipated rapidly in less than four wave periods (Anis and Moum, 1995, Kantha and Clayson, 2004, Paskyabi and Fer, 2014). Stokes production can be a very contribution to TKE, Kantha et at. (2010b, see also Kantha and Clayson 2004 and Kantha 2010a) estimated that its magnitude can be of the same order of conventional shear generated TKE and can extend deep into the water column where the shear generated by Stokes drift is still significant. Langmuir circulation cab extend vertically down to the mixed layer depth (Grant and Belcher,2009, Teixeira and Belcher, 2010).

In the collected dataset collected not all the information are available to fully investigate and scale the role of waves in turbulence generation. To give a general description of the relationship between different turbulence forcings we adopt a regime diagram (Li et al., 2005) as modified by Belcher et al. (2012). The diagram is constructed by plotting the Langmuir number versus the ratio of the buoyancy and wave forced turbulence. The Langmuir number La (McWilliams et al., 1997) represents the ratio between the wind and wave forced TKE production and is computed as

$$La = \left(\frac{u_*}{Us} \right)^{1/2} \qquad (9)$$

being *Us* the Stoke drift velocity. La = 0.35 (McWilliams et al. 1997) or La = 0.4 (Belcher et al., 2012) are common values for well developed sea and show a dominance of Langmuir circulation over wind forced production. The transition between those two regimes can be set for La = 0.7 (Belcher et al., 2012). The second ration is computed from the *Langmuir stability length* L_L:

$$L_L = \frac{-w_{*\mathrm{L}}}{J_b} \qquad (10)$$

where *Jb* is the buoyancy flux as computed in section 2.1 and w_{xL} is the scaling for wind and wave forced turbulence:

$$w_{*\mathrm{L}} = \left(u_*^2 Us\right)^{\frac{1}{3}} \qquad (11)$$

in which Us is the Stokes drift computed as descibed in section 2.1.

4 Yoyo casts and turbulence observations

Microstructure profiles were collected form a free falling profiler and hence the surface layer (roughly 2 meters) was lost. Moreover the usual practice in processing microstructure casts is to ignore depths up to twice the vessel draft in order to avoid contamination from the turbulent ship wake. However TKE dissipation profiles will be shown cutting off only the first 5 meters (roughly the vessel draft) because, even if noisy and not scaling well with the available forcing, data collected from 5 to 10 m can still give some information on the magnitude of the surface TKE production and on its transfer to deeper layers of the shallow GoT.

In the CARPET2014 dataset the observed TKE dissipation scaled as expected with the exception of a surface layer that can reach as deep as 10 meters (as TKE dissipation rate profiles in Figure 9 will show), this mismatch can be attributed to the complex forcing of surface turbulence. Figure 5 shows the regime diagram of turbulence forcing at Vida buoy computed every half an hour. A reduced time series (from February 2nd 00:00 UTC to February 4th 12:00 UTC) had to be chosen since it was the only period covered by the shipborne WASS observations, used to verify the JONSWAP spectrum, and of almost constant wind forcing. Up to the end of Y03 (February 3th at 12:00 UTC, green squares in figure 5) turbulence generation was dominated by wave forcing with some contribution from wind shear and a growing importance of buoyancy (the ratio h/L_L is slowly increasing). The orange squares

represent values between the end of Y03 and February 4th at 12:00 UTC and show a progressively weakening of all forcing with buoyancy decreasing to a lesser extent and hence defining a dominance of convection In TKE generation.

The regime diagram of Figure 5 gives as a general picture a condition in which the role of buoyancy in TKE generation changes significantly (h/L_L varies between 0.16 to 7.95), reaching a quasi dominance after Y03. Instead the values of *La* present much smaller variations (between 0.47 and 0.55), meaning that the relative contribution of wind and waves is almost constant throughout observations with a stronger role of the latter. During the following analysis we will show the similarity scaling for wind shear and buoyancy but not for waves due to the fact that no wave field observations were collected during the yoyo casts. Moreover using the probe in a free falling configuration we do not have information on the layer under direct influence of waves TKE production. Similarly not enough observations were collected to describe the eventual insurgence of Langmuir circulation. Hence, as will be discussed for Figure 9, there is a significant discordance between the observed profiles and the similarity scaling for the upper 10 m, this can be explained by the role of waves and wave-current interaction in generating and distributing turbulence. In this work we focus on the role of bottom intrusions with different turbidity in suppressing turbulence and hence we leave to future works a through description of the surface condition.

Yoyo cast Y01 ~~is~~was located in a shallower part of the GoT closer to the coast (Figure 1, red square in left panel). It presented~~s~~ a completely ~~well-~~mixed water column with no visible stratification and just a small increase in temperature (less than 0.2 °C) and a decrease in salinity (about 0.1 ~~psu~~) toward the end of the yoyo series (Figure 6). During sampling, ~~with surface salinities are over 37 psu,~~ surface salinity (well over 37) ~~data~~ shows no influence of the Isonzo ~~river~~River~~.~~; ~~The~~ turbidity levels, however, were significantly high, in the range of 22.6 to 23.5 FTU. TKE dissipation rate profiles showed high values near the sea surface, which progressively decreased to values of the order of 10^{-6} W kg^{-1} near the bottom, with one exception being the cast Y01-05 (fifth ensamble of yoyo Y01) in which ε values ~~are~~were high throughout the water column. ADCP-measured currents (Figure 7, lower panel green line) showed generally low bottom currents of magnitudes below 0.1 m s^{-1} with an increase toward the end of observations to values ~~just short~~

~~of~~smaller than 0.2 m s^{-1}. This can be explained by the change in tidal regime from falling to rising tide and is also reflected in the ε profiles that show an increase near the sea floor for the last ensembles of the series ~~)8(Figure~~ . The shallower cell (Figure 7, upper panel green line) presents a similar condition, with two peaks of magnitude just ~~short of~~less than 0.2 m s^{-1} but without an increasing trend~~e~~ during sampling. Current directions (Figure 7, black lines) are more ~~complicated~~complex, with dominant direction from the east for the surface cell, and from the southwest for the bottom cell.

The TKE dissipation rate profiles support measurements just described and are ~~also~~ in agreement with the local forcing (Figure 8). In the case of Y01-01 and Y01-07, both characterized by strong~~er~~ wind forcing, ~~dissipation rates fall around~~a surface layer of about 8 m in which TKE dissipation rates fall to 10^{-6} W kg^{-1} ~~at around 8 m depth~~, can be identified, while near the sea floor, the bottom shear stress did~~does~~ not ~~seem to~~ influence~~d~~ the TKE dissipation rate much. The Y01-08 ensemble was collected under weak winds and the surface layer with marked ~~resulting~~ TKE dissipation rate drop ~~reaches low values at~~ was shallower ~~depth~~, just ~~below~~ 5 m. The last ensemble of the series (Y01-11) was collected during rising tide with bottom currents up to 0.2 m s^{-1} and moderate wind stress. This is reflected in the TKE dissipation rate profile with a decrease with depth in the first 10 m and then a~~n~~ marked increase in the last 5 m, due to the influence of turbulence generated by the bottom shear stress. In all cas~~te~~s, the contribution of buoyancy-generated turbulence is weak (ε_b, magenta dashed line in Figure 8~~5~~) since the buoyancy flux is low and the Monin-Obukhov length scale is very large (negative), larger than the local sea floor depth (Figure 2, panel d). Y01 profiles show that in the absence of water column stratification, the ε profile is mostly defined by the surface wind and bottom stresses. ~~In this case, the turbulence generation due to buoyancy can be neglected, since the buoyancy flux is low and the Monin-Obukhov length scale is very large (negative) and larger than the local sea floor depth (Figure 2, panel d).~~

Yoyo casts Y02 and Y03 ~~are~~were located at the same site (Figure 1, blue square) but roughly two days apart from each other and ~~therefore~~ present significant differences in both water column structure and ε profiles. The w~~W~~ater column ~~observations collected~~ during Y02 (Figure 9) was always stratified, at the beginning of the casts

~~show a change in stratification, from a condition~~ with colder and fresher waters at the surface (~~coherent~~consistent with the influence of the Isonzo ~~river~~River discharges, as ~~supported~~hinted by high turbidity)~~.~~ then ~~to a condition~~ with warmer and saltier intrusion ~~water masses~~ near the sea floor. ~~S~~Higher suspended sediment concentrations ~~increase~~were observed at the bottom at the beginning and towards the end of the yoyo. Apart from the surface layer, the TKE dissipation rate ~~is~~was generally low from~~at~~ mid-depths to the sea floor with values almost at noise level (ε values lower than 10^{-8} W kg^{-1}), but increase~~d~~s by two orders of magnitude around 18:00 UTC of February 1st and then ~~again~~ decrease~~d~~s again to very low values. ADCP currents (Figure 1~~0~~1) at bottom (ADCP cell 3 cent~~e~~ered at 13 m depth, lower panel) and mid depths (ADCP cell 2 centred at 9 m depth, top panel) ~~are~~were similar, with water flowing to the northeast (current speed up to 0.2 m s^{-1}) during a rising tide up to around 20:00 UTC ~~with currents reaching 0.2 m s^{-1}~~. Once the tidal phase changes to falling tide, currents turn toward southeast, with a~~n~~ ~~pronounced~~abrupt change in the bottom layer, and drop to values below 0.05 m s^{-1}.

In contrast to the Y01 dataset, Y02 ensembles ~~have~~had a more complex behaviour due to the presence of surface stratification, the incoming water bottom intrusion~~mass~~ and the change in tidal character. ~~The first ensemble c~~Casts Y02-01 and Y02-04 (Figure 8, middle panels) ~~have~~had a similar water column structure, with fresher and cooler waters at the surface and more turbid waters near the sea floor. The surface wind stress ~~is~~was weak during both casts and a steep drop of ε to values below 10^{-6} W kg^{-1} can be seen around 7 m depth. Below this depth, the two ε profiles diverge due to different bottom current velocities. In Y02-01, ε falls to noise level due to a ~~much~~ slower bottom current (and hence low bottom shear stress) and higher turbidity that damps ~~wind-generated~~ turbulence in the water column. In contrast, ~~in~~ Y02-04~~,~~ was characterized by higher wind stress with TKE dissipation rate ~~was~~ significantly higher, reaching values above 10^{-6} W kg^{-1} with a profile that follows closely the ε_{sb}. In the second half of the yoyo series, wind speed increased up to values around 10 m s^{-1} which results in a deepening of the ε drop from 7 m to 10 m and 15 m in Y02-06 and Y02-10 respectively. Y02-06 has a bottom current velocity close to that of Y02-04~~,~~ but ~~the resulting~~ ε reaches lower values at the bottom due to the damping effect of the incoming water mass intrusion.

A more extreme case of an abrupt drop in TKE dissipation rate near the sea floor ~~is~~was Y02-10, in which ε reache~~d~~ds noise levels just 5 m above the sea floor. This ~~is~~was the result of concurrence of two factors. On the one hand, a sudden drop in bottom current velocity can be related to the change in the tidal character (that results in a lower ε_{sb}). On the other hand, a different water mass (warmer, saltier and with high concentrations of suspended sediments) intrude~~d~~ds in the bottom layer and acte~~d~~ds as a physical barrier to the propagation of wind-generated turbulence to the bottom part of the water column. The turbulence generated by buoyancy flux ~~is~~was low throughout ~~yoyo~~ Y02 with the exception of the first ensembles, as shown by the small Monin-Obukhov length (Figure 2).

Y03 (Figure 9, right panels) present~~ed~~s a water column ~~colder~~cooler and fresher than Y02 with values closer to Y01. ~~There is n~~No surface salinity stratification was observed as a result of the strong Bora winds that pushed the Isonzo plume out of the GoT along its northern shore and enhanced vertical mixing to a point in which the water column was completely mixed (i.e. Y03-07) ~~and tend to push the Isonzo plume out of the GoT along its northern shore~~. Moreover, the Isonzo discharges during Y03 presented a ~~temporary~~ decrease in magnitude from the ~~massive~~ flood event (mean discharge 500 m^3 s^{-1})~~. The mean discharge~~ lasting between noon of February 3rd and February~~Febraury~~ 4th~~was 500 m3 s-1~~. During Y03 ~~Near the sea floor,~~ two intrusions ~~are~~were observed near the bottom ~~(both in temperature and salinity); visible~~ one right at the beginning of the series ending at about 16:00 UTC, and one starting around 00:00 UTC and lasting for the remaining part of the yoyo. Even though those intrusions involve water masses of similar temperature and salinity, they ~~are~~were significantly different in turbidity, with the first intrusion ~~being more turbid~~carrying more suspended sediments than the second one. This can be partially ~~ascribed~~attributed to current speed and direction, with the first intrusion flowing south-west at velocities higher than 0.1 m s^{-1} and the second one due east at a much lower speed (Figure 10) with water properties consistent with~~. Considering water mass characteristics, the second intrusion shows water masses that are coherent with~~ an open sea origin as shown in Figure 5. It is of interest to note the abrupt change in current direction around 00:00 UTD right at the beginning of the second intrusion, which also points toward a different origin of this water mass.

Y03 ~~turbulent kinetic energy~~TKE dissipation rates ~~are~~were generally higher than those of Y02 throughout the series. Y03-01 ~~presents~~had a stratified water column with gradients across the pycnocline similar to those of ~~that is similarly stratified as that during~~ Y02-10~~(gradients across the pycnocline were of similar magnitude)~~ , with a mixed surface layer and with intruded turbid and dense water at bottom. Below the mixed surface layer, the ε value drop~~s~~eds to almost 10^{-8} W kg^{-1} at the top of the intrusion (20 m) and then abruptly rose ~~srise~~back to values of the order of 10^{-6} W kg^{-1} as a consequence of high bottom currents (Figure 8). In the case of Y03-07, there is no intrusion and ~~hence no pycnocline~~the water column is fully mixed, so that the ε profile after decreasing in the surface layer ~~stays~~stayed around ~~in the range of~~ 10^{-6} W kg^{-1} also near the sea floor (i.e. no significant influence of ε_{sb}.~~throughout the water column.~~ In the second part of the yoyo series (Y03-18 and Y03-20), ~~the arrival of~~ the intruding water mass ~~develops a density that,~~in contrast to Y03-01 and Y02-10, ~~is~~was not enhanced by a high suspended sediment load and hence the TKE dissipation rate ~~is~~was still damped by density interface but to a lesser degree than in the other cases.

5 Summary and discussion

Between the end of January and the first week of February 2014, during a period of high river discharges and moderate wind forcing, we were able to ~~collect~~make the very first microstructure measurements in the Gulf of Trieste. These observations, along with CTD casts, ADCP currents and meteorological measurements, provided a comprehensive picture of the effect of different forcing and water masses on the penetration of turbulence from its source regions and ~~therefore,~~ on mixing in the water column.

The CARPET2014 data set analysis shows a winter circulation inside the GoT driven mostly by wind, tides and the Isonzo River plume. As expected, a significant correlation was found between the bottom circulation, and the wind and tidal forcing. During strong wind periods, such as during Y02 or the beginning of Y03, bottom currents increased in magnitude, while during weaker winds, such as the beginning of Y02 and the end of Y03, they tended to decrease. Near the sea floor, two type of bottom water intrusion were identified: the first one coming from the Northern Adriatic coastal area during Y02 and the second one from the open sea in front of the Po

Delta during Y03. Those intrusions present similar densities but different physical properties (i.e. temperature and salinity) and suspended sediment concentration. Moreover, their arrival in the GoT followed periods dominated by different wind forcing, mostly Scirocco for the first intrusion and Bora for the second.

~~The θ-S diagram (Figure 5) shows that the GoT has salinity values close to or just smaller than those of the Northern Adriatic Sea waters, even during a period of high discharge of the Isonzo river. This can be explained by the interaction between different forcings: i) the moderate Scirocco and Bora winds that tend to keep the plume confined to the northern coast and push it due west, outside the Gulf; ii) the generally negative heat fluxes (from -150 W m^{-2} to -400 W m^{-2}), that result in a net buoyancy loss from the sea surface (Benetazzo et al., 2014); iii) the vertical mixing inside the GoT that, in absence of intruding water masses, tends to keep the water column mixed.~~

~~In the period covered by observations, the GoT was subject to moderate winds, with two calm periods in-between and a change in wind direction from southwestern Scirocco to northeastern Bora, and moderate heat fluxes (Figure 2). Bottom circulation appears to be influenced by winds both in magnitude and direction: during strong winds periods, such as during Y02 or the beginning of Y03, bottom currents increase in magnitude, while during weaker winds, such as the beginning of Y02 and the end of Y03, they tend to decrease (Figure 10). Bottom current velocities are also influenced by tidal phases with rising tides having an enhancing effect, as shown by the marked decrease at Y02 right after the tidal change, even under wind forcing in the order of 10 m s^{-1} (Figure 4).~~

~~The general circulation of the GoT is cyclonic with waters entering the Gulf from its southeastern coast and outflowing along the northern shore. The bottom waters observed during Y02 and Y03 have different end points, a condition that suggests two different origins. In the case of Y02, higher temperature and turbidity observed are consistent with waters coming from the northern coast of the Adriatic Sea, while clearer and colder waters of Y03 have an open sea origin. It is important to note that, even though the two origin sites are close to each other, these two water masses have different physical characteristics and so have a different impact on the turbulent kinetic energy dissipation rate profiles once they enter the GoT.~~Apart from the

surface layer, the TKE dissipation rates follow ~~closely~~ the similarity scaling for wind stress generated turbulence and for the one due to bottom shear stress near the sea floor (Figure 8). Buoyancy-driven turbulence under those conditions proved to be generally ~~not~~ insignificant, as ~~also~~ shown by the Monin-Obukhov length scale~~, which is almost always~~ beeing generally greater than the sea floor depth. ~~The behaviour of the dissipation rate under stronger heat fluxes, such as those observed in February 2012 (Benetazzo et al., 2014), could be significant, but has not yet been investigated.~~

The ε profiles of Figure 8 and the water column properties showed in Figures 6 and 9 can help in defining a general description of the impacts of density interfaces on the TKE dissipation rate in the water column. Specifically:

- Well-mixed water column: The TKE dissipation rate profile, below the surface layer, is solely defined by its forcing. Example of this are the Y01 ensembles, in which the ε profiles closely follow the scaling both in the middle of the water column and at depth (figure 8, top panels), and the Y03-07 ensemble which presented an almost constant TKE dissipation rate below the surface layer;
- Surface stratification: In presence of a stronger surface density interface (i.e. casts Y02-01 and Y02-04) turbulence is confined to the shallow surface layer with low ε values in the rest of the water column if bottom currents are low (Y02-01) or with an increase in ε in presence of strong bottom currents (Y02-04). It is noteworthy that in both cases the bottom turbidity was high but not able to damp turbulence in tha absence of a density interface.
- Dense bottom intrusion with turbidity gradient: When a turbidity gradient is also present at a density interface the damping effect on turbulence is significantly enhanced as in Y02-06, Y03-02 and Y02-10. In the first two ensembles an increase of ε was observed due to a strong bottom current which was not present during Y02-10, hence the sudden drop of O(2) in ε just below the density and turbidity interface;
- Denser bottom intrusion without any turbidity gradient: The presence of a density interface at the bottom produces a gradual damping of turbulence (Y03-18 and Y03-20). In this case, there is no significant difference in turbidity

between the intrusion and the ambient waters and hence ε is decreased but to a lesser degree than in the previous case.

~~in the case of Y02-10, ε does not increase after the interface because of higher concentration of suspended sediments, in contrast to Y03-02 that with similar ε_{sb} values but lower sediment concentration shows an increase of ε up to 10^{-6} W kg^{-1}.,Turbulence dissipation rate profiles throughout the campaign indicated values higher than 10^{-6} W kg^{-1} in the near-surface layers, then decrease up to two order of magnitude in the mid water column. In casts with strong bottom currents (i.e. Y01-11 or Y02-04), with the exception of the intrusion in Y02, dissipation rates tend to increase back to values of 10^{-6} W kg^{-1} near the sea floor due to the bottom stress. Anyway, this is a feature that has not been observed in the Adriatic Sea, mostly because observations used in previous studies did not reach the sea floor.~~

~~In our observations, apart from surface and bottom stresses, the water column structure (both the presence of buoyancy interfaces and suspended sediments) proved to be also important in determining the TKE dissipation rate. The profiles collected during the three yoyo casts can help in drawing a general picture. The first yoyo cast (Y01) shows a simple condition with a well-mixed water column, no interfaces and moderate wind forcing. Under these conditions, TKE dissipation rate profiles are defined mostly by the surface and bottom stresses, and turbulence can penetrate into the water column. Under weak bottom currents, such as at the beginning of Y01 series (Figure 7), ε profiles generally show a linear decrease from the sea surface to about 8 m (Figure 8, top row) and then a profile that follows the similarity scaling for ε_s to the bottom, as in the case of Y01-07. With higher bottom currents above the sea floor, as for Y01-11, ε starts to increase toward values higher than 10^{-6} W kg^{-1}, similar to those observed in surface waters.~~

~~The yoyo series Y03, in contrast to Y01, presents a water column with different stratification conditions. At the beginning of the series (Figure 9), a denser and more turbid intrusion near the bottom cause, as shown in cast Y03-02 (Figure 8, bottom panels), a steep drop of ε to almost noise levels just above the intrusion upper limit. The presence of stronger bottom current increases ε to values in the proximity of 10^{-6} W kg^{-1}, almost reversing the damping effect of the intrusion interface and bringing back the ε profile to a distribution similar to Y02-07, in which the intrusion is not~~

present. In Y03-18 and Y03-20, a different intrusion, with similar density but almost no turbidity (since it is clearer than previous intrusions) has a much smaller damping effect on ε.

The case of Y02 is more complex, and when compared to Y03, shows the role of buoyancy interfaces and suspended sediment concentrations in decreasing turbulence kinetic energy dissipation rates. Y02-01 has a water column with no density interface but with higher turbidity near bottom that results in a stronger damping of turbulence and low values of ε near the sea floor (Figure 8). A similar condition is present in Y02-04 but ε_{sb} values are higher, with a strong increase of ε values near the bottom of the water column. In both these cases, there are turbidity interfaces similar to that of Y03-02 but no density interface. It has to be noted that both Y02-01 and Y02-04 present a surface density interface that dissipates some of the TKE in the first few meters of the water column, hence reducing the amount of turbulence that can penetrate to the sea floor.

A more complex ε profile can be observed in cases in which both density and turbidity interfaces are present at the bottom. In the case of Y02-06, which is subject to a surface density interface, ε decreases in the first 10 m from the surface. Then it decreases to noise levels and rises again near the sea floor following the contribution of ε_{sb}. In this case, ε is not damped by the density and turbidity interface near the sea floor due to the fact that in its proximity it is already near noise levels. Instead in the case of Y02-10 the surface dissipation is weaker (there is no near surface interface) and ε keeps values around 10^{-6} W kg^{-1} up to the upper depth of the intrusion where it gets damped to values almost two order of magnitude lower. Comparison between the two profiles suggests that a strong interface (both in density and suspended sediments) damps turbulence in its vicinity. Moreover

The general picture that can be drawn from these results is that the water column structure (both the presence of buoyancy interface and suspended sediments gradients) hasplays a fundamental role to play in defining the TKE dissipation rate profiles, not only inside the interior of the water column but also in the proximity of the sea floor. In the specific case of the GoT, under moderate wind forcing, the presence of the intruding Adriatic Waters can be a significant limitation on complete mixing of the water column.

~~Due to contamination from the R/V *Urania*, the first 5 m from the sea surface was not considered in analysing the microstructure data collected. But these depths represent a fundamental part of turbulence generation and propagation since they are affected not only by wind but also by waves. In order to fully understand these processes, in future studies, this part of the water column should be investigated using a profiler rising from the bottom sufficiently far away from the ship, instead of a falling profiler deployed from the side of the vessel.~~

Appendix A

The traditional approach in processing microstructure profiles~~to reach statistical significance and increase the accuracy~~ calls for averages of repeated casts (~~in practice,~~when logistically feasible three or more) at each station, to reach statistical significance and increase the accuracy~~.~~ The averaging produces meaningful results for the mean profiles and yields quantities more representative of the turbulence in the water column. However, cases in which the water column has strong stable density interfaces moving up and down are exceptions. In those cases, turbulence and other parameters differ from one cast to another in their vicinity. In the CARPET 2014 dataset, changes in the interface depth between casts ~~are~~were as much as 4 m. This means that by averaging measured quantities at fixed depths over consecutive profiles, the averages ~~are~~get smeared, and hence characterized by smoother gradients and broader peaks. To avoid this, an ad-hoc algorithm was developed using the central profile of each ensemble as reference and realigning sections of the remaining profiles to it. The mean profile was then obtained by averaging the central profile with the realigned sections. The step-by-step procedure applied to two consecutive vertical profiles, is as follows:

1. One profile is chosen as the reference (Figure 3 panel a, cyan) and the other as the one to be realigned (Figure 3 panel a, black).
2. Starting from the surface the correlation coefficients are computed for a progressively longer section, until the full profiles (i.e. surface to bottom) are accounted for. Starting from the surface, the section with the maximum correlation value is considered as a "surface layer" that doesn't need to be shifted. In Figure 3 panel b, its lower limit is the horizontal red line.

3. The root mean square error for remaining parts of the profiles is then computed with a 5 point moving window (Figure 3, panel c red line) and the maximum peaks are found (Figure 3, panel c red dots)~~.,~~ ~~il~~ If the two peaks are closer than 10 points to each other, just the largest one is considered. The 10-point window was chosen because in a sensitivity test (not shown), it proved to be the most efficient in separating the two peaks. The two peaks are then used to identify the sections to realign. The limit of each section is set at the midpoint between two peaks (black lines, in Figure 3).
4. Each section of the profile to be realigned is then correlated to the reference profile shifting it from +20 to -20 points. The shift with maximum correlation is then taken as the needed shift. In Figure 3 panel d, the reference profile is in cyan, the one to be shifted in black and the shifted sections are in red.

The process is repeated for each successive cast at the station and then the averages are computed over the new shifted profiles and the reference one. Figure A1~~3~~ shows the original profiles (left panel, red: reference, green: profile one and blue: profile 3), their conventional mean in black, the shifted profiles and their mean (central panel, same colours) and the two means (right panel, original mean in cyan and shifted mean in black). Figure A1~~3~~ also presents the same plots but for ε.

The method described above offers a more meaningful vertical distribution of the TKE dissipation rate, by taking into account the vertical oscillations of the pycnocline, since turbulence is extinguished in the vicinity of strongly stable interfaces. As a consequence, in the vertically shifted profiles, the peaks in the TKE dissipation rate are much clearer and better represent the shape of the observed profiles. The peaks are just above the thermocline. In general, when more than one cast is collected at a station, the most conservative assumption is to consider the central profile as the reference one for the water column structure. Other profiles over the cycle are then realigned with respect to the reference profile to obtain the TKE dissipation rate caused by vertical shear, uncontaminated by the zero values right at the interface.

Acknowledgements

The authors thank~~s~~ CNR-UPO for having ~~allowed~~granted R/V *Urania* ship time, and the vessel crew is thanked for their kind cooperation. CARPET2014 campaign was supported by the Flagship Project RITMARE - The Italian Research for the Sea –

coordinated by the Italian National Research Council and funded by the Italian Ministry of Education, University and Research within the National Research Program 2011–2013. This work was also supported by the FP7 project COCONET (Grant Agreement No: 287844) of the European Commission.

References

Anis, A. and Moum J.N.: Surface wave-turbulence interactions: Scaling (z) near the sea surface. J. Phys. Oceanogr, 25(9), 2025 – 2045, 1995.

Benetazzo, A., Fedele, F., Gallego, G., Shih, P.-C., Yezzi, A.: Offshore stereo measurements of gravity waves. Coast. Eng. 64, 127–138.

Benetazzo, A., Graham, L., Carniel S.: Mapping Coastal Frontal Zones In Northern Adriatic via AUV. Sea Tech.,

Belcher S.E. and others: A global perspective on Langmuir turbulence in the ocean surface bounday layer. Geo. Phys Lett., 39, L18605, doi: 10.1029/2012GL052932, 2012.

Burchard H. and others: Observational and numerical modeling methods for quantifying coastal ocean turbulence and mixing. Prog. Oceanogr. 76(4),399-442, 2008.

Carniel S., Sclavo M., Kantha L. and Prandke H.: Double-diffusive layers in the Adriatic Sea. Geophys Res Lett, 35, L02605, doi:10.1029/2007GL032389, 2008.

Carniel S., Kantha L.H., Book, J.W., Sclavo M. and H. Prandke: Turbulence variability in the upper layers of the Southern Adriatic Sea under a variety of atmospheric forcing conditions. Cont. Shelf Res., 44,39-56, 2012.

Comici, C., and Bussani A.: Analysis of the River Isonzo discharge (1998-2005), Bolletino di Geofisica Teorica ed Applicata, 48(4), 435-454, 2007.

Csanady, G. T. (1982). Circulation in the Coastal Ocean, 279 pp., D. Reidel, Dordrecht.

D'Asaro, E.: Turbulence in the upper-ocean mixed layer. Annu. Rev Marine. Sci., 6,101 115, 2014.

Falcieri, F.M., Benetazzo, A., Scalvo, M., Russo, A.,Carniel, S.: Po River plume pattern variability investigated from model data. Cont. Shelf Res., 87(15), 84 – 95, 2013. doi:10.1016/j.csr.2013.11.001.

Fairall, C.; Bradley, E.; Hare, J. and Grachev A.: Bulk parameterization of Air-Sea fluxes: updates and verification for the COARE algorithm. J. Climate, 16, 571 – 591, 2003.

Gargett, A.E.: “Theories” and techniques for observing turbulence in the euphotic zone. Sci Mar, 6(suppl. 1), 24-45, 1997.

Grant, L.A. and Belcher, S.E.: Characteristics of Langmuir turbulence in the ocean mixed layer.J Phys Oceanogr, 39, 1871 – 1997, 2009.

Gregg, M.C.: Dynamic mixing in the thermocline: a review. J. Geophys. Res, 32, 5249 – 5286, 1987.

Hasselmann, K.: Wave-driven inertial oscillations. Geophys Fluid Dyn, 45, 55 – 62, 1970.

Hasselmann, K., Barnett, T.P., Bouws, E., Carlson, H., Cartwright, D.E., Enke, K., Ewing, J.A. Gienapp, H., Hasselmann, D.E., Kruseman, P., Meerburg, A., Müller, P., Olbers, D.J., Richter, K., Sell, W., Walden, H.: Measurements of wind-wave growth and swell decay during the Joint North Sea Wave Project (JONSWAP). Deutches Hydrographisches Institut, 1973.

Kantha, L.K.: Turbulent entrainment at a buoyancy interface due to convective turbulence. In Freeland, H.J., Farmer, D.M., Levings, C.D. (Eds.), Fjord Oceanography. Plenum Press, 205 – 2015, 1980.

Kantha, L. H.: A numerical model of Arctic leads, J. Geophys. Res., 100, 4653-4672, 1995.

Kantha L.H. and Clayson C.A.: Small Scale Processes in Geophysical Fluid Flows. Academic Press, vol. 67, 2000.

Kantha L.H. and Clayson C.A.: On the effect of surface gravity waves on mixing in the oceanic mixed layer, Ocean Modelling, 6, 101-124, 2004.

Kantha, L., Lass, H. U., Prandke, H.: A note on Stokes production of turbulence kinetic energy in the oceanic mixed layer: observations in the Baltic Sea. Ocean Dyn., 60, 171-180, 2010a.

Kantha, L.: Modeling turbulent mixing in the global ocean: second moment closure models. In Turbulence: Theory, Types and Simulation, ed. R. J. Marcuso, Nova Science Publishers, 1-68, 2010b.

Li M., Gargett, C., Skyllingstad, E.: A regime diagram for classifying turbulent large eddies in the upper ocean. Deep-Sea Res Pt.I, 52, 259 – 278, 2005.

Malačič, V., and Petelin B.: Gulf of Trieste, in Physical Oceanography of the Adriatic Sea, Past, present and Future, edited by B. Cushman-Roisin, M. Gačić, P.-M. Poulain and A. Artegiani, pp. 167-177, Kluwer Academic Press, Dordrecht, 2001.

Malačič, V., Celio M. and Naudin J.J.: Dynamics of the surface water in the Gulf of Trieste (Northern Adriatic) during drifting experiments, paper presented at Ecosystem research report No 32- the Adriatic Sea - Proceedings of the workshop 'Physical and biogeochemical processes in the Adriatic Sea', Office for Official Publications of the European Communities, Luxembourg, Portonovo, 23-27 April 1996, Italy.

Malačič, V., Petelin B., and Vodopivec M.: Topographic control of wind-driven circulation in the northern Adriatic, J. Geophys. Res., 117(C6), C06032, doi: 10.1029/2012jc008063, 2012.

McWilliams, J.C., Sullivan P.P., Moeng, C.H.: Langmuir turbulence in the ocean. J. Fluid. Mech., 94(C4), 6273 – 6284, 1997.

Paskyabi, M.B., Fer, I.: Turbulence structure in the upper ocean: a comparative study of observations and modelling. Ocean Dynam, 64, 611 – 631, 2014.

Prandke, H., Stips, A.: Test measurements with an operational microstructure-turbulence profiler: Detection limit of dissipation rates. Acqua Sci., 60, 191 – 209, 1998.

Prandke H., Holtsch K. and Stips A.: MITEC Report Technical Note No. I.96.87, European commission, Joint Research Center, Sapce applications Institute, ISPRA/Italy (2000).

Peters H. and Orlić M.: Turbulent mixing in the springtime central Adriatic Sea. Geofizika, 22, 2005

Peters H., Craig M.L., Orlić M and Dorman C.E.: Turbulence in the wintertime northern Adriatic Sea under strong atmospheric forcing. J Geophys Res., 112, C03S09, doi: 10.1029/2006JC003634, 2007.

~~Querin S., Crise A., Deponte D. and Solidoro, C.: Numerical study of the role of wind forcing and freshwater buoyancy input on the circulation in a shallow embayement (Gulf of Trieste, Northern Adriatic Sea). J Geoph Res, 111, C03S16, doi:1029/2006JC003611, 2006.~~

~~Raicich M.: On the fresh water balance of the Adriatic Sea. J Mar Sys, 9, 305 – 319, 1996.~~

Ricchi A., Miglietta M.M., Falco P.P., Benetazzo A., Bonaldo D., Bergamasco A., Sclavo M., Carniel S.: On the use of a coupled ocean-atmosphere-wave model during an extreme Cold Air Outbreak over the Adriatic Sea, Atmos Res, in review.

Shay, T.J. and Gregg M.C.: Turbulence in an oceanic convective mixed layer, Nature, 310, 282 – 285, 1984.

Shay, T. J., and Gregg M.C.: Convectively driven turbulent mixing in the upper ocean, J. Phys. Oceanogr., 16, 1777– 1798, 1996.

~~Sinjur, I., G. Vertačnik, L. Likar, V. Hladnik, I. Miklavčič, and Gustinčič M.: Ice storm in Slovenia in January and February 2014 - Spatial and temporal variability in weather across the dinaric landscapes in Slovenia. In Slovenian, abstract and discussion in English, Gozdarski vestnik, 72(7-8), 299-309, 2014.~~

Simpson, J.H., Bos, W.G., Shirmer, F., Souza, A.J., Rippeth, T.P.., Jones, S.D., Hydes, D.: Periodic stratification in the Rhine ROFI in the North Sea. Oceanologica Acta, 16 (1), 23 – 32. 1993.

Teixieira, M.A.C. and Belcher, S.E.: On the structure of Langmuir turbulence. Ocean Sci, 9, 597 – 608, 2010.

Thorpe, S.A.: Recent developments in the study of ocean turbulence. Annu Rev Earth Planet Sci, 32, 91-109, 2004.

Thorpe, S.A. (2005): The Turbulent Ocean. Cambridge University Press, Cambridge, UK, 439 pp.

Table 1 Specifics of each yoyo set. Times are in UTC.

Set	Starting time	Ending time	Ensembles (casts)	Intervals
Y01	30/01/2015 20:50	31/01/2015 02:30	11 (54)	30 minutes
Y02	01/02/2015 14:00	02/02/2015 01:40	12 (36)	30 minutes
Y03	03/02/2015 15:50	04/02/2015 04:11	27 (87)	15 -30 minutes

Table 21. BIAS, Root Mean Square Error (RMSE) and Percentual RMSE computed for the ISMAR and NIB MSS probes compared to CTD measurements.

	BIAS	RMSE	PRMSE
ISMAR – Temperature	0.0046	0.0205	0.1932
ISMAR – Salinity	-0.2418	0.2424	0.6517
NIB – Temperature	-0.0072	0.0280	0.2530
NIB – Salinity	0.030	0.2227	0.0607

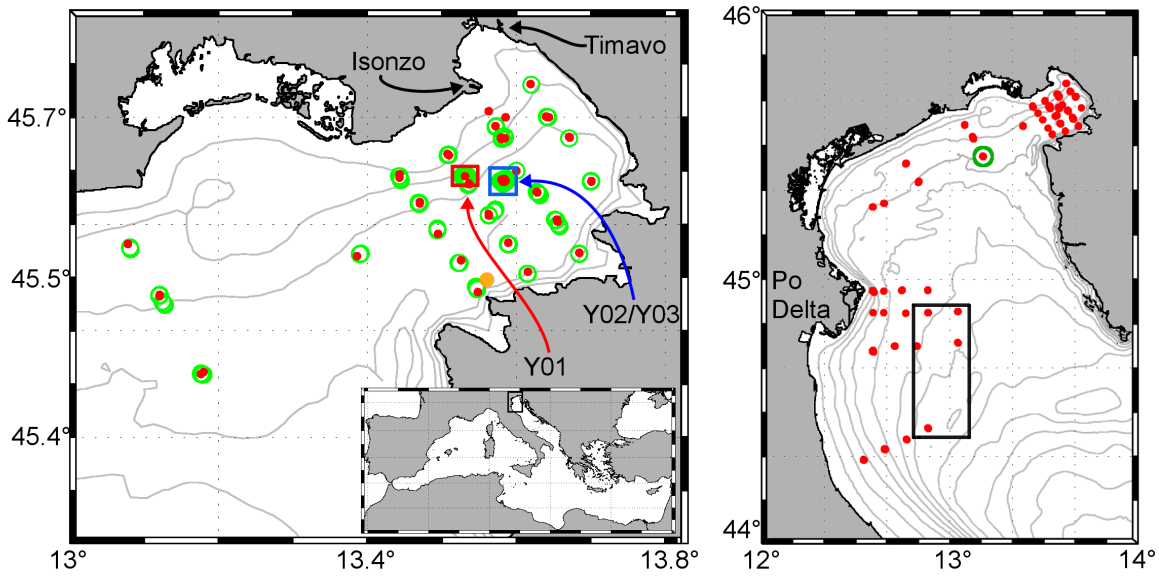

Figure 1. (lLeft panel) shows the lLocation of the CARPET2014 stations inside the GoT. Red dots denote CTD stations; green circles MSS stations, red and blue squares MSS yoyo sites fro Y01 and Y02/Y03 respectively; yellow dot points the VIDA buoy. The insert shows the location of the Adriatic Sea inside the Mediterranean Sea.

(4Right panel) shows sStations of the entire CARPET2014 cruise. Red dots show locations of CTD casts; black squarerectangle marks the area of the CTD casts considered representative of open sea waters (see Figure 5), the green circle shows the station used as Y02 and Y03 casts end points.

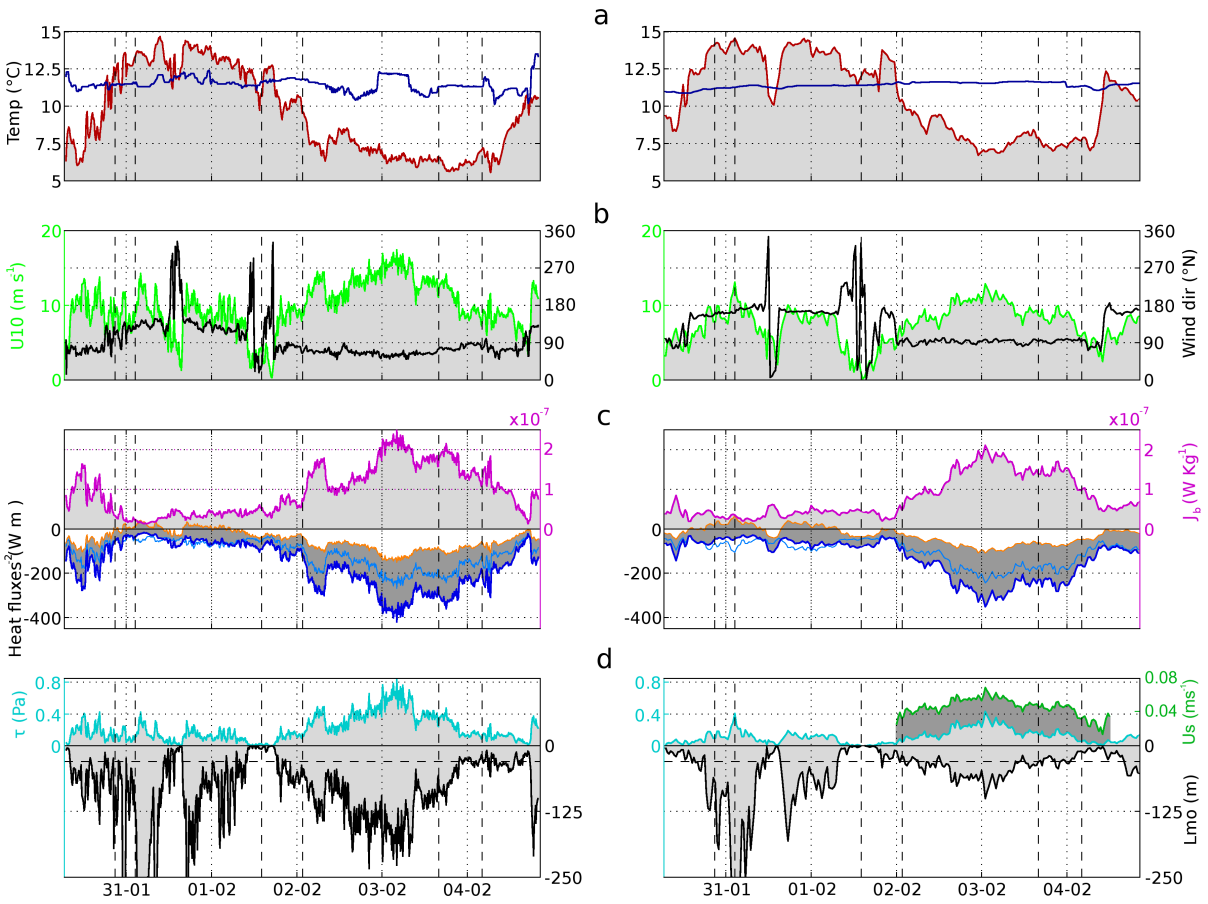

Figure 2. Atmospheric and sea surface observations and fluxes collected from the R/V *Urania* (left panels) and VIDA buoy (right panels). (a) Air (~~Tair,~~ red) and sea (~~Tsea,~~ blue) temperature time series; (b) wind speed (light green) and wind direction (black); (c) net (~~J_{to},~~ blue line), latent (~~J_l,~~ light blue) and sensible (~~J_s,~~ orange) heat fluxes computed with the COARE algorithm and buoyancy flux (~~J_b,~~ magenta); (d) wind stress (~~τ,~~ cyano), ~~and~~ Monin-Obukhov length (~~L_{mo},~~ black) and Stokes drift (dark green). Given that the maximum depth of the GoT is 25 m, ~~the~~ L_{mo} is shown up to -250 m depth to provide a clearer representation of the water column. L_{mo} values can be as ~~much~~low as -1200 m during ~~the~~ calm periods. Vertical dashed lines show the yoyo cast collection time.

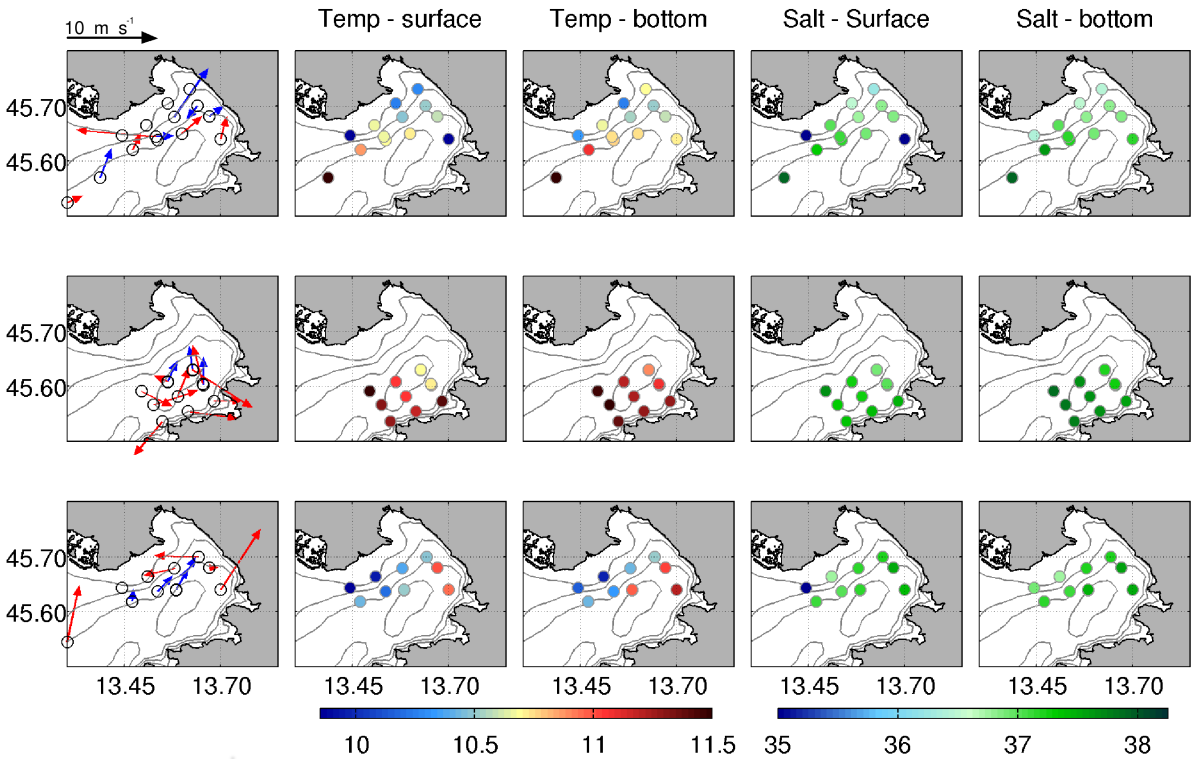

Figure 34: Bottom currents and values from CTD casts at ~~certain~~surface and bottom ~~depths~~ are shown inside the GoT for January 30th (top panels), January 31st (central panels) and February 4th (bottom panels). Panels on the left column show the ADCP bottom cell currents; red arrows are observations taken during rising tide, blue arrows during falling tide. Temperature (second and third columns) and salinity (fourth and fifth columns) values are shown for surface (0 and 2.5 m) and bottom layers (last 2.5m of cast) inside the GoT.

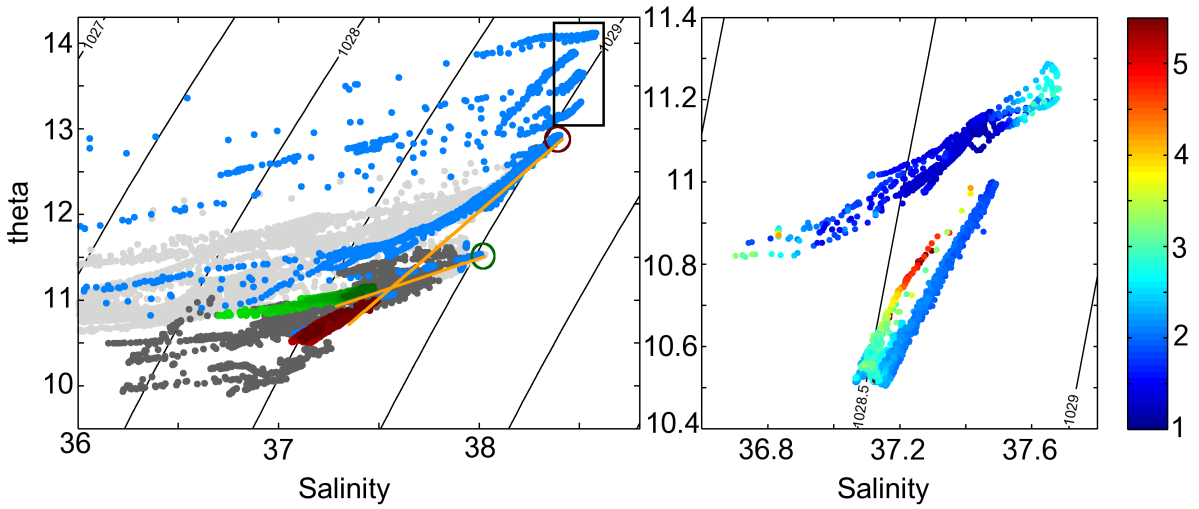

Figure ~~45~~. ~~(L~~left panel~~)~~ ~~shows~~ θ-S plot of all CTDs and MSSs (both ISMAR and NIB) ~~observations~~casts (light grey for the Northern Adriatic and dark grey for the GoT). The green and red dots are the MSS-ISMAR and MSS-NIB ensemble means for Y02 and Y03 respectively, light colour for surface values and dark colour for bottom ones. The green circle indicates the bottom waters observed at the entrance of the GoT on January 30th that are the end point for Y02 bottom waters; Red circles point to deep waters outside the GoT on January 4th considered as the end point of Y03 bottom water. The black square encompasses values in bottom waters in the centre of the North Adriatic Sea. Locations of end points are shown in Figure 1. The profiles of the cast leading to the end points are shown in light blue.

~~R~~(right panel)~~ows sh~~ θ-S plot for Y02 and Y03. Colour scale shows turbidity FTUs as measured by the back scatterometer mounted on the MSS ISMAR probe.

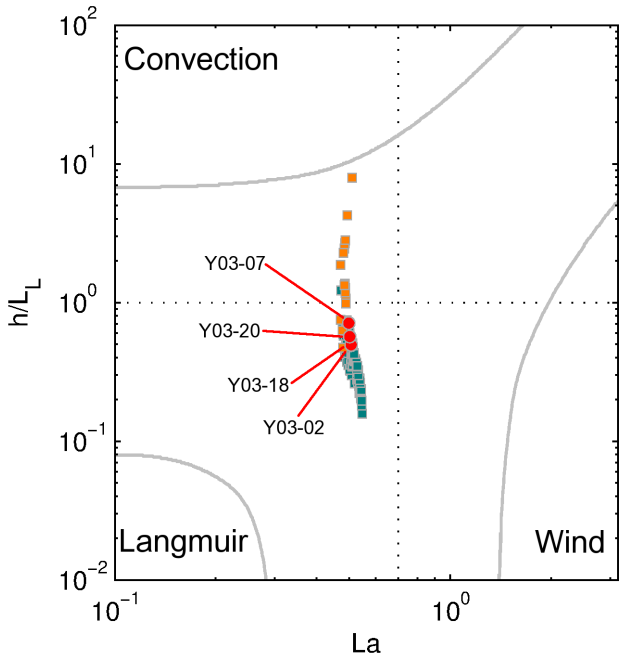

Figure 5 Regime diagram of turbulence forcing computed at the VIDA buoy from February 2nd (14:30 UTC) to 4th (12:00 UTC). Green and orange squares represents values before and after the Y03, red marks are the values for the ensembles shown in Figure 9. The horizontal dashed line indicates the demarcation between convection dominated turbulence and shear stress dominated one; the vertical dashed line shows demarcation between conventional wind stress driven turbulence and Stokes production driven one.

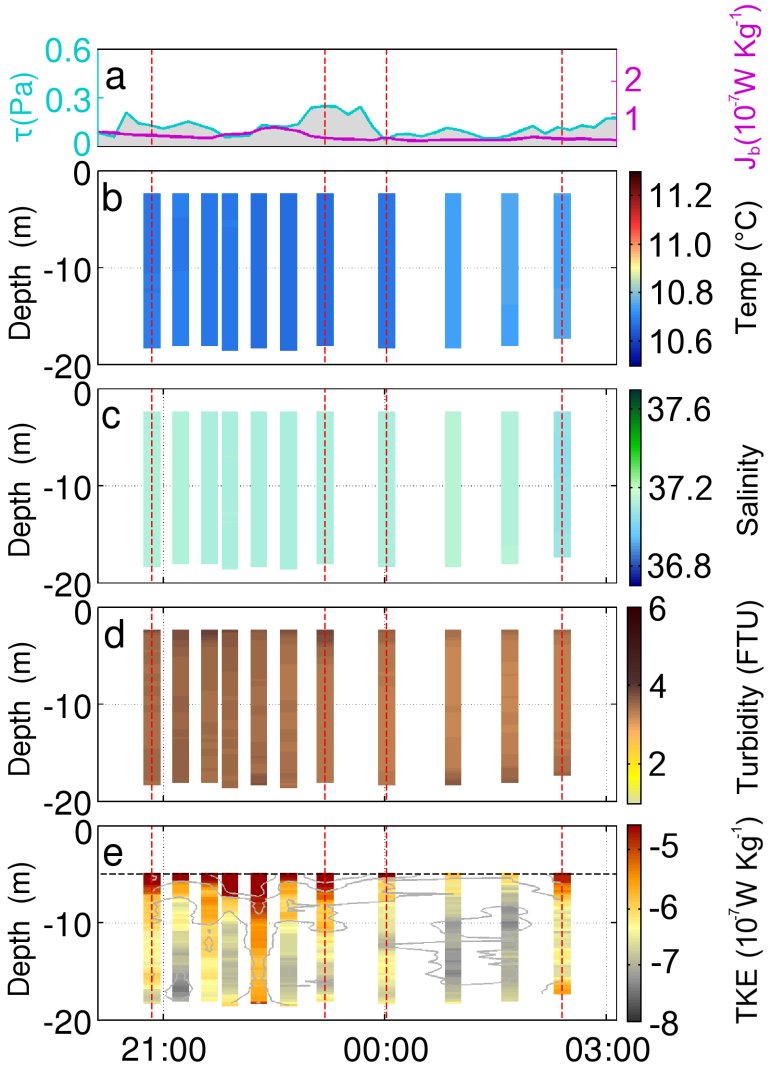

Figure 6: Hovmöller diagrams for Y01: a) wind stress and buoyancy flux during the Y01, b) temperature profiles; c~~b~~) salinity profiles; d~~c~~) turbidity profiles in FTU; e~~d~~) turbulent kinetic energy dissipation rate in logarithmic scale (contours spaced in log of 1 W Kg^{-1}). Red dashed lines show the time of collection of the Y01 casts reported in top panels of Figure 8.

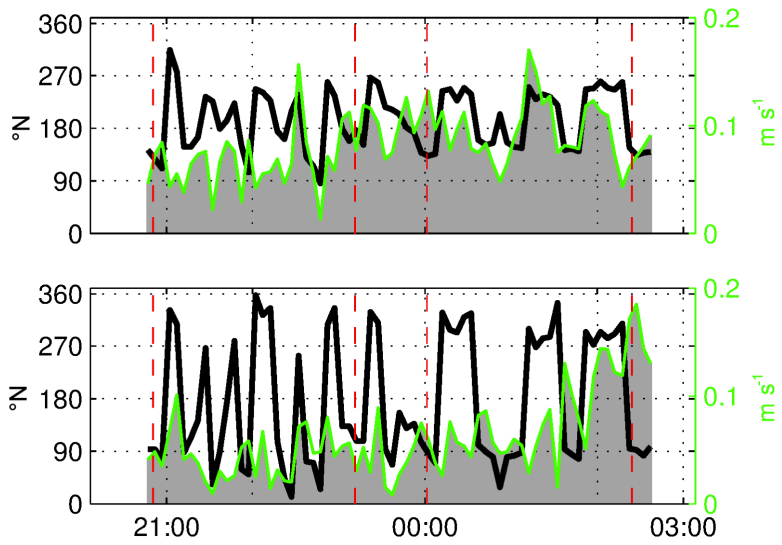

Figure 7: Y01 ADCP currents: ~~S~~second (top panel) and third (bottom panels) cells of Y01 ADCP currents. The cell centres are located at 13 m and 17 m below sea surface; cell width is 4 m. Black lines show current direction in degrees (due north) and green lines show current magnitude in m s^{-1}. Red dashed lines show the time of collection of the Y01 casts reported in top panels of Figure 8.

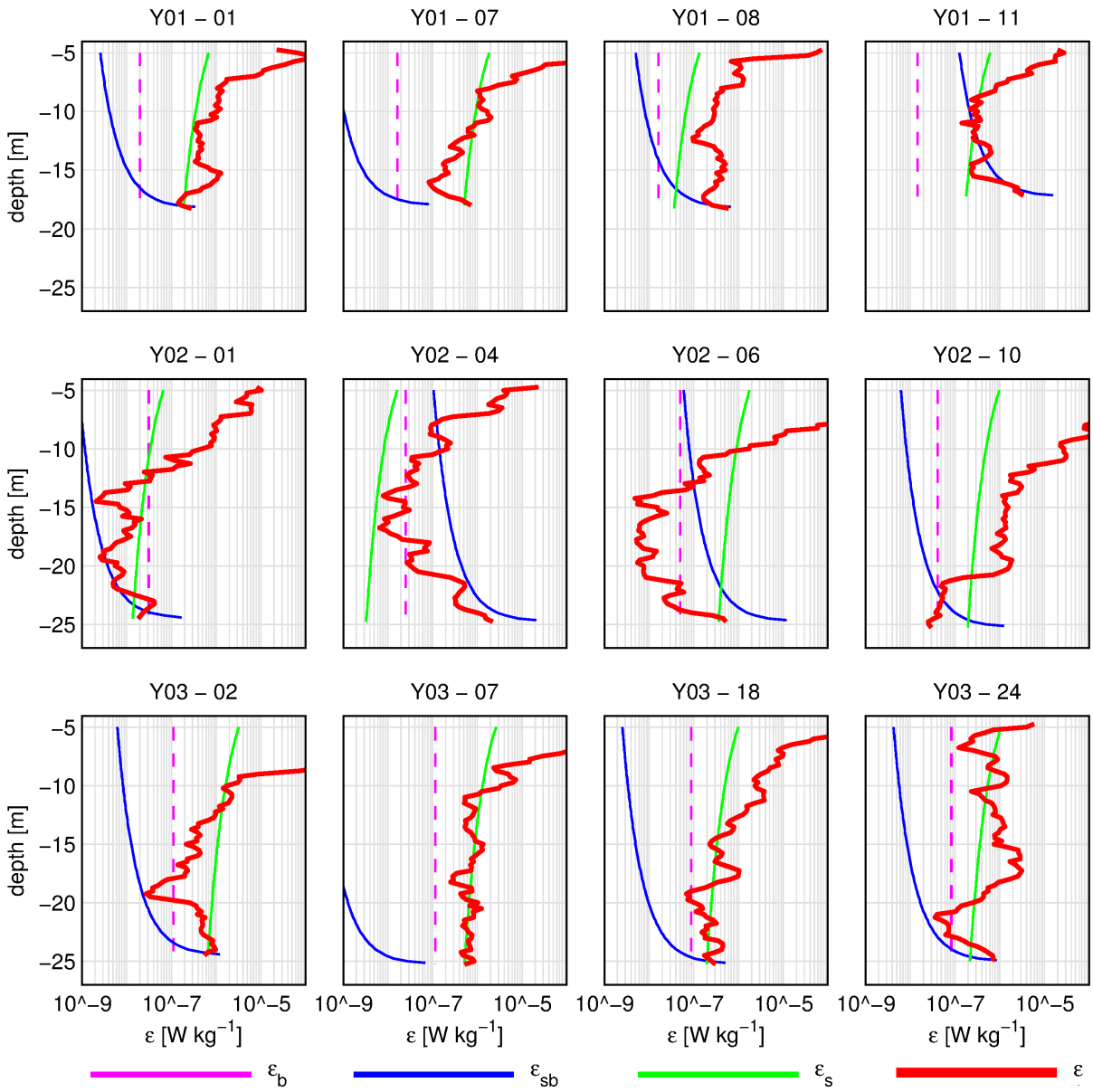

–Figure 8: Similarity scaling of turbulent kinetic energy dissipation rate (ε) for four representative casts for each yoyo, Y01 top panels, Y02 central panels and Y03 bottom panels. For each cast is shown the observed TKE dissipation rate (ε, thick red line), and the turbulence generated by surface wind stress (ε_s, green line), bottom shear stress (ε_{sb}, blue line) and buoyancy flux (ε_b, magenta vertical dashed line).

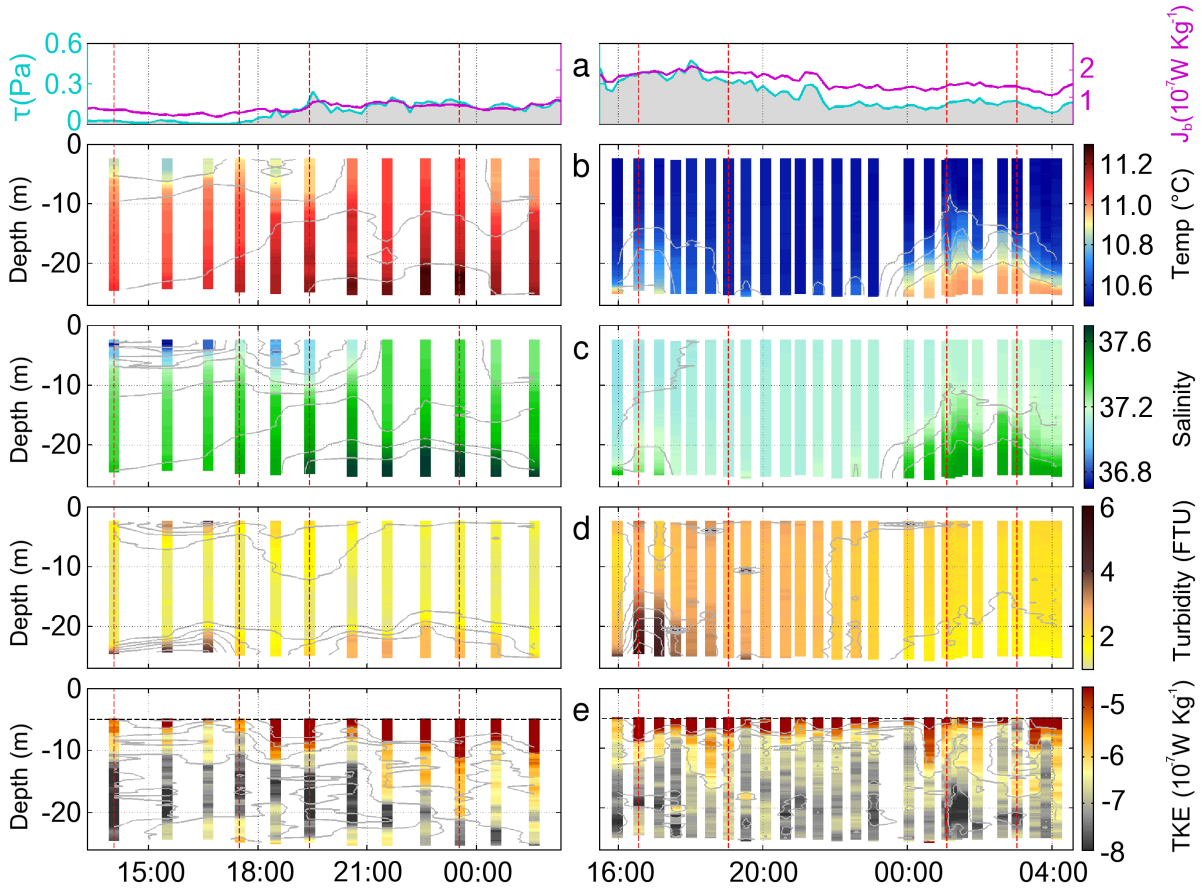

Figure 9. Hovmöller diagrams of Y02 (left) and Y03 (right). Panels shows: a) wind stress (cyan) and buoyancy flux (magenta); ba) temperature profiles (grey contours are spaced 0.1 °C); cb) salinity profiles (grey contours are spaced 0.1 ~~PSU~~); dc) turbidity profiles in FTU (grey contours are spaced 1FTU); ed) turbulent kinetic energy dissipation rate in logarithmic scale (contours spaced in log of 1 W m^{-2}). Red dashed lines show the time of collection of the Y01 casts reported in top panels of Figure 98.

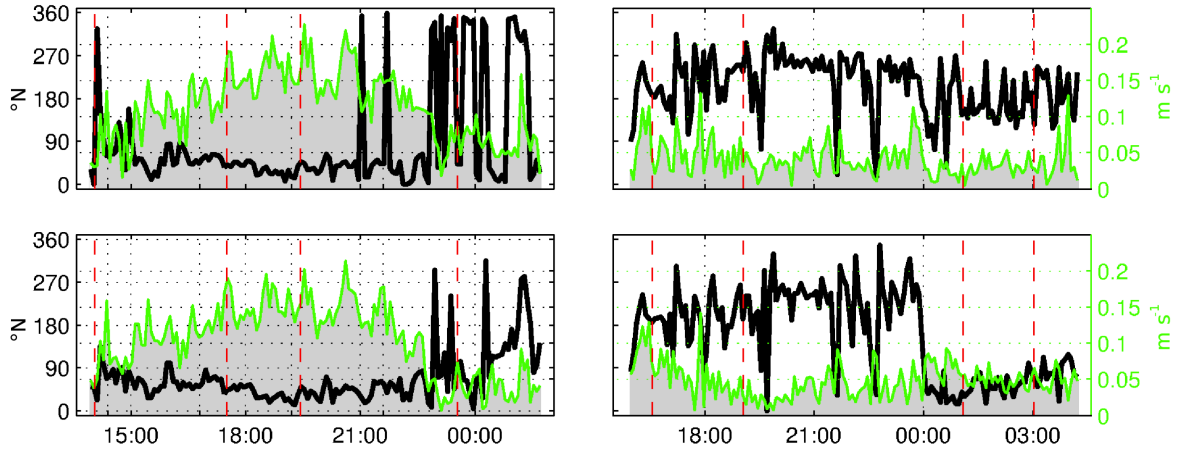

Figure 10: Second (top panel) and third (bottom panels) cells of ADCP currents. The cell centres are located at 13 m and 17 m below sea surface; cell width is 4 m. Black lines show current direction (due north) and green lines show current magnitude in m s^{-1}. Left panels show Y02, right panels Y03. Red dashed lines show the time of collection of the Y01 casts reported in top panels of Figure 9~~8~~.

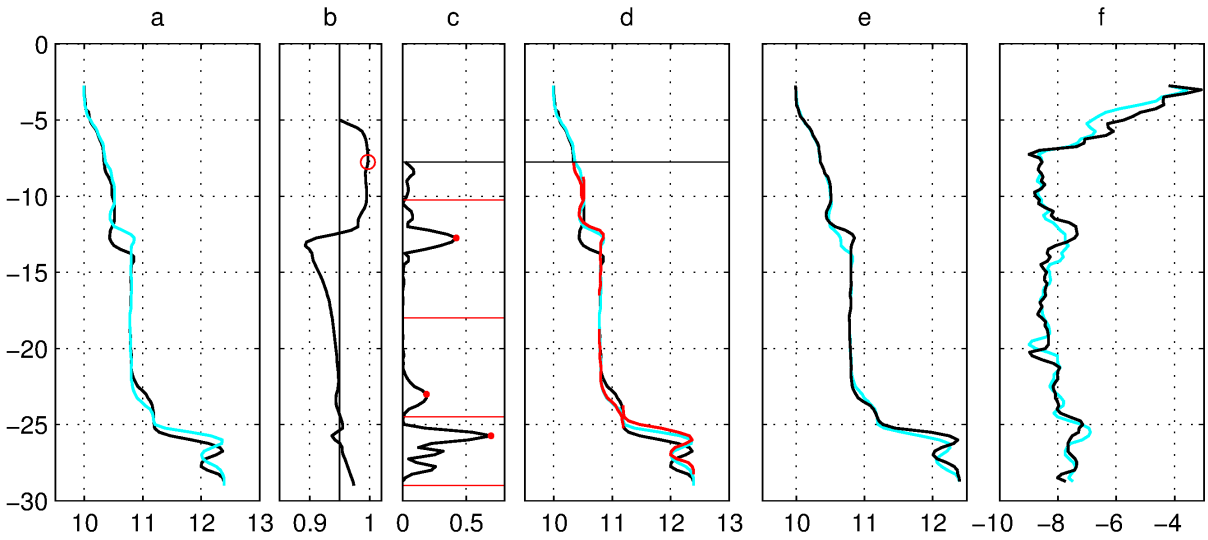

Figure A1. Panel a: original temperature profiles used in the realignment algorithm: reference in cyan, profile to be realigned in black. Panel b: correlation coefficient computed for progressively longer segments starting form surface. The black vertical line is the 0.95 correlation threshold and the red circle the maximum correlation. Panel c: root mean square error between the two profiles; red dots identify peaks. Black horizontal lines divide the segments used for realignment. Panel d: the realigned segments (thin red lines) above the two original profiles. Panels e and f show the mean profile for temperature and turbulent kinetic energy dissipation rates computed using the original profiles (cyan) and the realigned ones (black).